JGS
Journal of the Geological Society

Perspective

https://doi.org/10.1144/jgs2020-222 | Vol. 179 | 2022 | jgs2020-222

A template for an improved rock-based subdivision of the pre-Cryogenian timescale

Graham A. Shields[1*], Robin A. Strachan[2], Susannah M. Porter[3], Galen P. Halverson[4], Francis A. Macdonald[3], Kenneth A. Plumb[5], Carlos J. de Alvarenga[6], Dhiraj M. Banerjee[7], Andrey Bekker[8], Wouter Bleeker[9], Alexander Brasier[10], Partha P. Chakraborty[7], Alan S. Collins[11], Kent Condie[12], Kaushik Das[13], David A. D. Evans[14], Richard Ernst[15,16], Anthony E. Fallick[17], Hartwig Frimmel[18], Reinhardt Fuck[6], Paul F. Hoffman[19,20], Balz S. Kamber[21], Anton B. Kuznetsov[22], Ross N. Mitchell[23], Daniel G. Poiré[24], Simon W. Poulton[25], Robert Riding[26], Mukund Sharma[27], Craig Storey[2], Eva Stueeken[28], Rosalie Tostevin[29], Elizabeth Turner[30], Shuhai Xiao[31], Shuanhong Zhang[32], Ying Zhou[1] and Maoyan Zhu[33]

[1] Department of Earth Sciences, University College London, London, UK
[2] School of the Environment, Geography and Geosciences, University of Portsmouth, Portsmouth, UK
[3] Department of Earth Science, University of California at Santa Barbara, Santa Barbara, CA, USA
[4] Department of Earth and Planetary Sciences, McGill University, Montreal, Canada
[5] Geoscience Australia (retired), Canberra, Australia
[6] Instituto de Geociências, Universidade de Brasília, Brasilia, Brazil
[7] Department of Geology, University of Delhi, Delhi, India
[8] Department of Earth and Planetary Sciences, University of California, Riverside, CA, USA
[9] Geological Survey of Canada, Ottawa, Canada
[10] School of Geosciences, University of Aberdeen, Aberdeen, UK
[11] Department of Earth Sciences, The University of Adelaide, Adelaide, Australia
[12] New Mexico Institute of Mining and Technology, Albuquerque, NM USA
[13] Department of Earth and Planetary System Sciences, Hiroshima University, Hiroshima, Japan
[14] Department of Earth and Planetary Sciences, Yale University, New Haven, CT, USA
[15] Department of Earth Sciences, Carleton University, Ottawa, Canada
[16] Faculty of Geology and Geography, Tomsk State University, Tomsk, Russia
[17] Isotope Geosciences Unit, S.U.E.R.C., East Kilbride, UK
[18] Institute of Geography and Geology, University of Würzburg, Würzburg, Germany
[19] Department of Earth and Planetary Sciences, Harvard University, Boston, MA, USA
[20] University of Victoria, Victoria, Canada
[21] School of Earth and Atmospheric Sciences, Queensland University of Technology, Brisbane, Australia
[22] Institute of Precambrian Geology and Geochronology, R.A.S., St. Petersburg, Russia
[23] Institute of Geology and Geophysics, Chinese Academy of Sciences, Beijing, China
[24] Centro de Investigaciones Geológicas–CONICET–FCNyM, (UNLP), La Plata, Argentina
[25] School of Earth and Environment, University of Leeds, Leeds, UK
[26] Department of Earth and Planetary Sciences, University of Tennessee, Knoxville, TN, USA
[27] Birbal Sahni Institute of Palaeosciences, Lucknow, India
[28] Department of Earth Sciences, University of St. Andrews, St. Andrews, UK
[29] Department of Geological Sciences, University of Cape Town, Cape Town, South Africa
[30] Laurentian University, Sudbury, Canada
[31] Department of Geosciences, Virginia Tech, Blacksburg, VA, USA
[32] Institute of Geomechanics, Chinese Academy of Geological Sciences, Beijing, China
[33] Nanjing Institute of Geology and Palaeontology, Nanjing, China

GAS, 0000-0002-7828-3966; SMP, 0000-0002-4707-9428; CJdA, 0000-0002-9676-5555; DMB, 0000-0003-4951-3360; ASC, 0000-0002-3408-5474; KC, 0000-0002-7743-9535; KD, 0000-0002-2372-2095; DADE, 0000-0001-8952-5273; AEF, 0000-0002-7649-6167; BSK, 0000-0002-8720-0608; SWP, 0000-0001-7621-189X; CS, 0000-0002-4945-7381; ES, 0000-0001-6861-2490; SX, 0000-0003-4655-2663; MZ, 0000-0001-7327-9856

* Correspondence: g.shields@ucl.ac.uk

Abstract: The geological timescale before 720 Ma uses rounded absolute ages rather than specific events recorded in rocks to subdivide time. This has led increasingly to mismatches between subdivisions and the features for which they were named. Here we review the formal processes that led to the current timescale, outline rock-based concepts that could be used to subdivide pre-Cryogenian time and propose revisions. An appraisal of the Precambrian rock record confirms that purely chronostratigraphic subdivision would require only modest deviation from current chronometric boundaries, removal of which could be expedited by establishing event-based concepts and provisional, approximate ages for eon-, era- and period-level subdivisions. Our review leads to the following conclusions: (1) the current informal four-fold Archean subdivision should be simplified to a tripartite scheme, pending more detailed analysis, and (2) an improved rock-based Proterozoic Eon might

comprise a Paleoproterozoic Era with three periods (*early Paleoproterozoic* or *Skourian*, Rhyacian, Orosirian), Mesoproterozoic Era with four periods (Statherian, Calymmian, Ectasian, Stenian) and a Neoproterozoic Era with four periods (pre-Tonian or *Kleisian*, Tonian, Cryogenian and Ediacaran). These proposals stem from a wide community and could be used to guide future development of the pre-Cryogenian timescale by international bodies.

Received 15 December 2020; **revised** 5 June 2021; **accepted** 7 June 2021

The term 'Precambrian', or more traditionally 'pre-Cambrian' (Glaessner 1962), is an informal geological term that refers to the time before the beginning of the Cambrian Period at *c.* 0.54 Ga (Peng *et al.* 2020). The two pre-Cambrian eonothems (Archean and Proterozoic) have long pedigrees (Sedgwick 1845; Logan 1857; Dana 1872) but were introduced formally only after extensive discussion among members of the Subcommission on Precambrian Stratigraphy (SPS), which was tasked with Kalervo Rankama as chair in 1966 to standardize Precambrian nomenclature (Trendall 1966). James (1978), summarizing discussions within the subcommission, outlined five categories of proposals: (1) subdivision by intervals of equal duration (Goldich 1968; see also Hofmann 1990, 1992; Trendall 1991); (2) subdivision by major magmatic-tectonic cycles (Stockwell 1961, 1982); (3) subdivision by stratotypes (Dunn *et al.* 1966; see also Crook 1989); (4) subdivision by breaks in the geological record defined by radiometric ages (James 1972); and (5) subdivision based on Earth evolution concepts (Cloud 1976). One result of those early discussions was that an approximate chronological age of 2500 Ma was assigned to a somewhat transitional Archean–Proterozoic boundary (James 1978). However, further subdivision of the Precambrian in a comparable manner to that achieved for younger rocks, although favoured by some (Hedberg 1974), proved unworkable (James 1978) due to (1) the relatively fragmentary nature of the Precambrian rock record, much of which is strongly deformed and metamorphosed, and (2) a scarcity of age-diagnostic fossils. For this reason, a mixed approach was applied: Global Standard Stratigraphic Ages (GSSAs) were introduced to subdivide Precambrian time, but the absolute ages of periods were chosen to bracket major magmatic-tectonic episodes (Plumb and James 1986; Plumb 1991). Since that decision was ratified, all of pre-Cryogenian Earth history and its geological record has been subdivided using geochronology rather than chronostratigraphy.

The principal Precambrian subdivisions now comprise the informal Hadean and formal Archean and Proterozoic eons (Fig. 1a), which, following the GSSA concept, are defined as units of time rather than stratigraphic packages. The Hadean Eon refers to the interval with no preserved crustal fragments that followed formation of the Earth at *c.* 4.54 Ga (Patterson 1956; Manhes *et al.* 1980). Because the Hadean Eon left no rock record on Earth (other than reworked mineral grains or meteorites), it cannot be regarded as a stratigraphic entity (eonothem) and has never been formally defined or subdivided. It is succeeded by the Archean Eon, which is usually taken to begin at 4.0 Ga and is itself succeeded at 2.5 Ga by the Proterozoic Eon. The Archean Eon is informally divided into four eras (Eoarchean, Paleoarchean, Mesoarchean and Neoarchean; e.g. Bleeker 2004*a*), although a three-fold subdivision is widely favoured (Van Kranendonk *et al.* 2012; Strachan *et al.* 2020). The Proterozoic Eon is currently subdivided into three eras (Paleoproterozoic, Mesoproterozoic and Neoproterozoic) and ten periods (Siderian, Rhyacian, Orosirian, Statherian, Calymmian, Ectasian, Stenian, Tonian, Cryogenian and Ediacaran). The era names were conceived after a proposal from Hans Hofmann in 1987 (Hofmann 1992; Plumb 1992), while the period names derive from discussions within the SPS (Plumb 1991). The three Proterozoic eras were originally proposed to begin at 2.5 Ga (Proterozoic I), 1.6 Ga (Proterozoic II) and 0.9 Ga (Proterozoic III), respectively (Plumb and James 1986). However, the beginning of the Neoproterozoic Era was subsequently moved to 1.0 Ga in the final proposal (Plumb 1991).

The ages of Precambrian boundaries were selected to delimit major cycles of sedimentation, orogeny and magmatism (Plumb 1991; Fig. 1a). However, knowledge has improved considerably over the past thirty years due to: (1) increasingly precise and accurate U–Pb zircon dating; (2) improved isotopic and geochemical proxy records of tectonic, environmental and biological evolution; and (3) new rock and fossil discoveries. As a result, some of these numerical boundaries no longer bracket the events for which they were named. The International Commission on Stratigraphy (ICS) began to address this problem in 2004 when they ratified the basal Ediacaran GSSP (Global Stratotype Section and Point) on the basis of the stratigraphic expression of a global chemo-oceanographic (and climatic) event in a post-glacial dolostone unit in South Australia (Knoll *et al.* 2004). Latest geochronology and chronostratigraphy confirm that all typical Marinoan 'cap dolostone' units were deposited contemporaneously at 635.5 Ma (Xiao and Narbonne 2020). The Ediacaran GSSP is therefore one of the most highly resolved system-level markers in the entire geological record.

The chronostratigraphic (re)definition of the Ediacaran Period (and System) replaced the provisional GSSA (650 Ma) that had been used to mark the end of the Cryogenian Period. This revision allowed the Marinoan 'snowball' glaciation (*c.* 645–635 Ma) to be included within the geological period that owed its name to that and Sturtian glaciations. The 850 Ma age marking the beginning of the Cryogenian was subsequently found to be much older than consensus estimates for the onset of widespread Sturtian 'snowball' glaciation at *c.* 717 Ma (Macdonald *et al.* 2010; Halverson *et al.* 2020), and so it was also removed, following a proposal from the Cryogenian Subcommission (Shields-Zhou *et al.* 2016). A globally correlative stratigraphic horizon at or beneath this level has not yet been proposed by the Cryogenian Subcommission, although an approximate placeholder age of *c.* 720 Ma for the boundary, pending a ratified GSSP, has been written into the international geological timescale (Fig. 1). Despite the lack of a GSSP, the age revision of the Cryogenian Period by 130 million years has been quickly accepted by the geological community worldwide, presumably because the new ages match better the natural phenomena for which it was named.

With respect to both the Cryogenian and Ediacaran GSSPs as well as the earlier ratification of the Precambrian–Cambrian boundary GSSP (Brasier *et al.* 1994), establishment of a rock-based or chronostratigraphic concept permitted relatively easy consensus around an approximate, stratigraphically calibrated age, before more prolonged and detailed discussions could take place towards eventual GSSP proposal and ratification. In the light of rapidly expanding knowledge about Precambrian Earth history, these three precedents serve to illustrate how the GSSA approach could be replaced by a more natural, chronostratigraphic framework (e.g. Bleeker 2004*a*, *b*; Van Kranendonk *et al.* 2012; Ernst *et al.* 2020). Identified shortcomings with the inflexible GSSA approach include: (a) a lack of ties to the rock record and broader Earth and planetary history; (b) the diachronous nature of the tectonic events on which the current scheme (Fig. 1a) is based; and (c) the lack of any major sedimentological, geochemical and biological criteria that can be used to correlate subdivision boundaries in stratigraphic

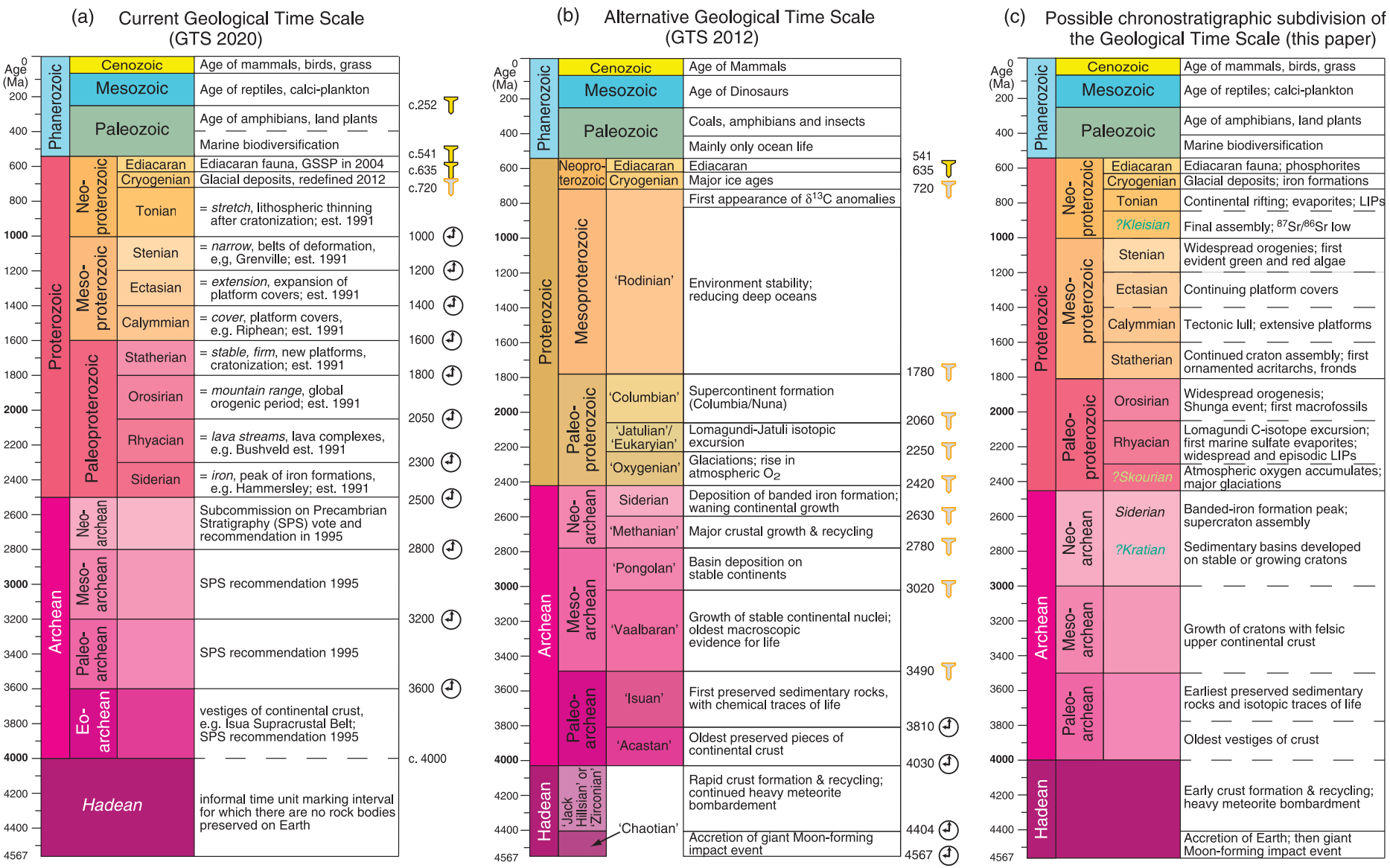

Fig. 1. (**a**) Current geological timescale (after Strachan *et al.* 2020). (**b**) Timescale proposal of Van Kranendonk *et al.* (2012) retaining original colour scheme. Golden spike symbols represent ratified (yellow) and potential (pale) GSSP levels. Clock symbols represent ratified Proterozoic and recommended Archean GSSAs. (**c**) Proposed chronostratigraphic subdivision of the geological timescale (this paper). (**a**–**c**) depict subdivisions of decreasing duration from left to right: eons, eras and periods. Note that era and period boundary ages are only approximate ages and would inevitably change in any internationally agreed chronostratigraphic scheme. Period names in italics represent suggested changes to existing nomenclature. If the first period of the Paleoproterozoic Era were renamed (here as the *Skourian* Period; cf. Oxygenian Period of Van Kranendonk *et al.* 2012), we recommend that the term 'Siderian' be retained for the final period of the Archean Eon.

records. The nomenclature of Proterozoic periods is thus commonly out of step with the concepts or phenomena for which they were named, while the underlying basis for both era and period nomenclature is neither universally accepted nor widely understood.

An alternative stratigraphic scheme for the Precambrian was therefore proposed by Van Kranendonk *et al.* (2012) based on potential GSSPs (Fig. 1b). Following the rationale of Cloud (1972), the approach taken was to base a revised Precambrian timescale as closely as possible around geobiological events, such as changes to oceans, atmosphere, climate or the carbon cycle that would be near instantaneous compared to changes in geotectonic processes. We agree with the rationale pursued by Van Kranendonk *et al.* (2012), which followed an earlier proposal of Bleeker (2004*a*), while noting that some newly proposed subdivisions represent a radical departure from standard practice. This is illustrated by the proposal of a new and exceptionally long 'Rodinian' Period between 1800 and 850 Ma (Van Kranendonk *et al.* 2012), which replaced five of the pre-existing Proterozoic periods. The principle of naming a geological period after a hypothetical supercontinent is not widely accepted.

In this contribution, we outline the geological basis behind current chronometric divisions, explore how boundaries might differ in any future chronostratigraphic scheme, identify where major issues might arise during the transition to that scheme, and propose where some immediate changes to the present scheme could be easily updated/formalized, as a framework for future GSSP development. We note that this is not only a matter of academic interest for geologists. Establishing a robust, coherent and intuitive stratigraphic nomenclature will be of great importance for improving understanding of Earth's history in schools, universities and the wider community.

The formal process of timescale definition

The International Commission on Stratigraphy (ICS), a constituent scientific body of the International Union of Geological Sciences (IUGS), is the formal international body that defines precisely global units (eonothems, erathems, systems, series, stages) of the International Chronostratigraphic Chart, that, in turn, are the basis for the units (eons, eras, periods, epochs and ages) of the International Geological Timescale. A total of 17 bodies of international experts (subcommissions) are tasked with achieving consensus subdivision of specific portions of Earth history, generally geological periods, that can then be ratified through voting by first ICS and then IUGS officers, leading to formal amendment of international geological timescale charts. Formal chronostratigraphic subdivision is eventually achieved through ratification of a specific, but globally correlative level in one sedimentary succession in the world, referred to as a 'golden spike' or more formally as a GSSP (Global Stratotype Section and Point). As mentioned above, a purely chronometric subdivision of Proterozoic time was ratified in 1991 (Plumb 1991), following an arduous process begun in 1966 (Trendall 1966). Although Archean GSSAs were agreed among members of a subsequent Precambrian Subcommission, and appear on international geological time charts, they have not been formally defined or ratified (Robb *et al.* 2004).

Following ratification of a chronostratigraphic definition and GSSP for the terminal Proterozoic Ediacaran Period in 2004 (Knoll *et al.* 2004, 2006*a*, *b*), the Neoproterozoic Subcommission (2004–12) was set up to explore further subdivision below the newly named system. This work resulted in the establishment of the Cryogenian and Ediacaran subcommissions in 2012, and formal ratification of a chronostratigraphic definition for the Cryogenian base in 2016 (Shields-Zhou *et al.* 2016). Further subdivision of pre-Cryogenian Neoproterozoic time was left jointly to the Precambrian and Cryogenian subcommissions, whereby in 2020 the Precambrian Subcommission formally changed its name to the Precryogenian Subcommission. Considering the exponential increase in stratigraphically relevant information pertaining to the pre-Cryogenian rock record, as well as the wide range of disciplines involved in its study worldwide, it no longer seems tenable to cover subdivision of 84% of Earth history within a single subcommission. The present authorship represents a wide-ranging working group, which was set up by the ICS in 2019 and tasked with preparing a formal proposal on how chronostratigraphic subdivision of pre-Cryogenian time might be expedited (Harper *et al.* 2019). A key part of this process will be the formal removal of all current pre-Cryogenian GSSAs by the IUGS, and their replacement by chronostratigraphically defined units, pending future discussion towards eventual GSSP ratification.

Transitioning from a purely chronometric to a chronostratigraphic scheme for pre-Cryogenian time will inevitably place more emphasis on the rock record and on precise stratigraphic levels within key successions and their global equivalents. In this regard, we accept the arguments made by Zalasiewicz *et al.* (2004) that units of time and strata are essentially interchangeable, once boundary stratotypes and GSSPs are defined. Specifically, we consider that it may not always be appropriate to use the terms eonothem, erathem or system (for packages of strata deposited during eons, eras and periods, respectively), considering the enormously long time intervals and relatively incomplete rock records of the pre-Cryogenian archive. As a consequence, we mainly use time subdivisions below (eons, eras, periods), while emphasizing that any future GSSPs would eventually need to be defined using a level within a globally correlative boundary stratotype section. Although the ages of period boundaries would change in a more closely rock-based or chronostratigraphic scheme, we support retention of all currently ratified period names. Existing period names, borrowed from the Greek, were chosen to delimit natural phenomena of global reach and we consider that any new global nomenclature ought to follow this lead for consistency. For this reason, we discourage the use of both supercontinent names and regional phenomena in future international nomenclature.

Recent progress towards, and widespread acceptance of, chronostratigraphic definitions for two Precambrian periods suggest that the international community can act expeditiously to address inadequacies of the chronometric scheme, while overcoming the confusion generated by the informal erection of new periods and unsupported concepts. Our intention here is to accelerate the removal of GSSAs by helping to frame rock-based concepts and establish approximate ages for eon-, era- and period-level subdivision of pre-Cryogenian time, pending eventual ratification of more detailed GSSP proposals.

Indicators of crustal, atmospheric and biological evolution: implications for the geological timescale

Recent research has focused on understanding episodicity and secular trends in the Precambrian geological record, recognizing that the supercontinent cycle and mantle dynamics exert a fundamental control on the evolution of not only the Earth's lithosphere, but also the atmosphere and biosphere, via a series of complex, incompletely understood feedbacks (e.g. Worsley *et al.* 1985; Lindsay and Brasier 2002; Bekker *et al.* 2010, 2014; Cawood *et al.* 2013; Young 2013; Grenholm and Schersten 2015; O'Neill *et al.* 2015; Hawkesworth *et al.* 2016; Van Kranendonk and Kirkland 2016; Gumsley *et al.* 2017; Nance and Murphy 2018; Alcott *et al.* 2019; Shields *et al.* 2019). Here we review recent developments in the understanding of a wide range of indicators of crustal, atmospheric and biological evolution and the attendant implications for division of the geological timescale.

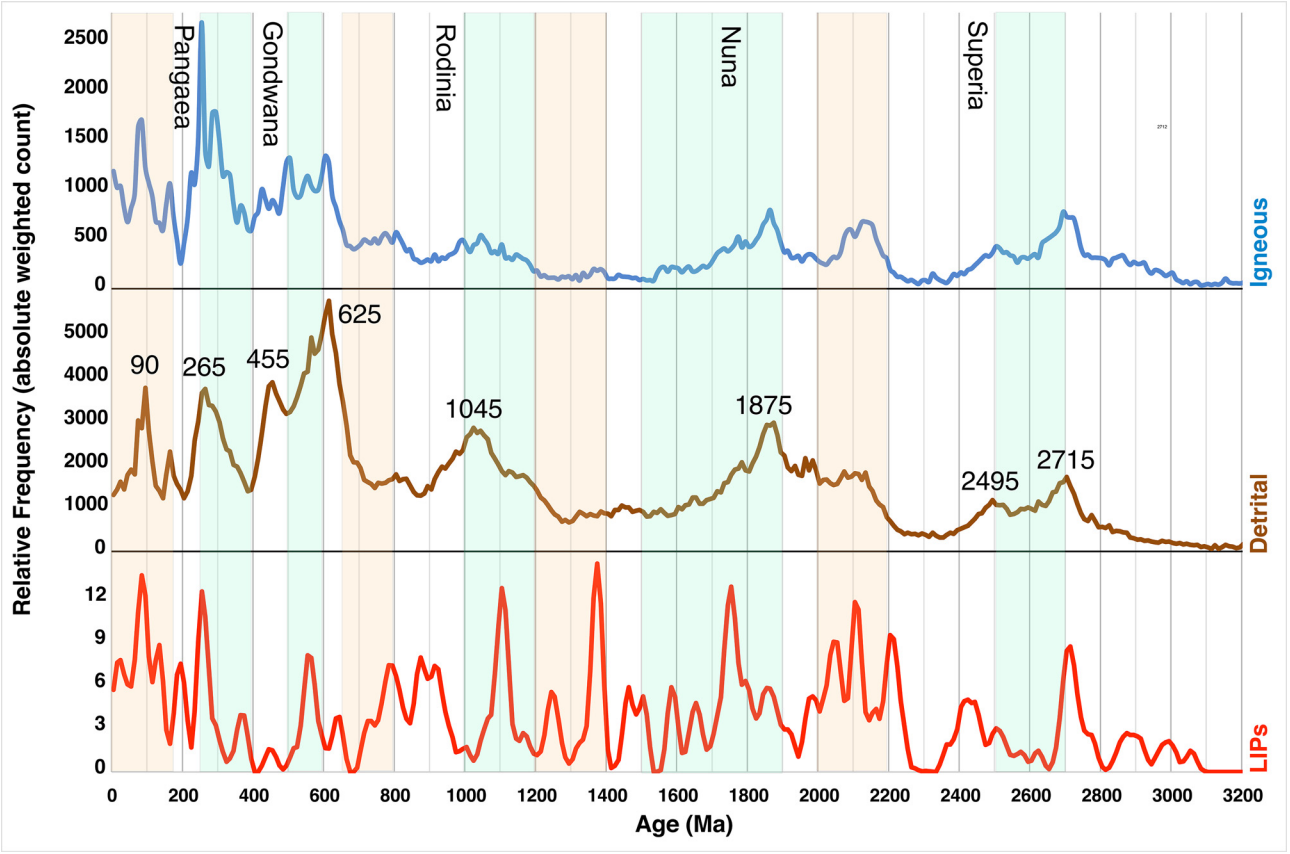

Fig. 2. Raw time-series plots from age histograms at 10 Ma intervals, regional weighting of ages, and U–Pb records accepted with absolute discordance <70 Ma and 2σ uncertainty <70 Ma (after Condie and Puetz (2019). (**a**) U–Pb igneous zircon ages ($n = 180\,412$); (**b**) U–Pb detrital zircon ages ($n = 501\,938$); (**c**) Large Igneous Province (LIP) ages represented by 535 crustal provinces (no regional weighting, smoothed with 3-weight Gaussian kernel). U–Pb zircon age peaks match intervals of supercontinent assembly (pale green), whereas troughs correspond to intervals of supercontinent tenure (generally white) and break-up (pale brown) (after Condie and Aster 2010; Condie 2014). Major current and proposed chronostratigraphic boundaries (Fig. 1c) at *c.* 2450, 1800, 1000, 540, 252 and 66 Ma follow zircon abundance peaks.

Tectonic processes and the supercontinent cycle

Various workers have proposed that the Precambrian can be subdivided on the basis of the dominant tectonic process at any one time. Hawkesworth *et al.* (2016) suggested five intervals: (1) initial accretion, core/mantle differentiation, development of magma ocean and an undifferentiated mafic crust; (2) plume-dominated tectonics (pre-subduction) at *c.* 4.5–3.0 Ga; (3) stabilization of cratons and onset of 'hot subduction' between *c.* 3.0 and 1.7 Ga; (4) the 'Middle Age' at 1.7–0.75 Ga; and (5) Rodinia break-up and development of 'cold subduction' from 0.75 Ga onwards. Similarly, Van Kranendonk and Kirkland (2016) suggested five intervals, each of which starts with a pulse of mafic–ultramafic magmatism, includes the formation of a supercontinent, and ends with an often-protracted period of relative quiescence as the previously formed supercontinent drifts and breaks apart. Following *c.* 4.03–3.20 Ga – the period from the start of the preserved rock record to the onset of modern-style plate tectonics – these stages are: (1) 3.20–2.82 Ga – the onset of modern-style plate tectonics and the oldest recognized Wilson cycle; (2) 2.82–2.25 Ga – commencing with major crustal growth, emergence of the continents and formation of Superior-type BIFs, and closing with magmatic slowdown and stagnant-lid behaviour; (3) 2.25–1.60 Ga – global mafic/ultramafic magmatism followed by global terrane accretion and the formation of Nuna; (4) 1.60–0.75 Ga – partial break-up of Nuna and subsequent formation of Rodinia during the Grenvillian and other orogenies; (5) 0.75 Ga to present – break-up of Rodinia, the Pangaean supercontinent cycle and present transition to Amasia (Mitchell *et al.* 2012; Safonova and Maruyama 2014; Merdith *et al.* 2019).

Worsley *et al.* (1985) and Nance *et al.* (1986) pointed out that processes associated with the supercontinent cycle can be tracked by several isotopic proxies. One proxy that has emerged since their pioneering studies relates to the U–Pb ages of zircon grains over the past 4.0 Ga. Compilations of U–Pb zircon ages obtained from orogenic granitoids and detrital sedimentary rocks record similar peaks, which correspond broadly to the times of global-scale collisional orogenesis and magmatism associated with the amalgamations of Superia, Nuna (Columbia), Rodinia, Gondwana and Pangaea supercontinents or supercratons, respectively (Mitchell *et al.* 2021). A recent compilation (Condie and Puetz 2019) interprets these peaks to be pulses of crustal growth and revises their timing to 2715, 2495, 1875, 1045, 625, 265 and 90 Ma (Fig. 2). A kernel density estimate analysis (Vermeesch *et al.* 2016) of almost 600 000 detrital zircon grains (Spencer 2020) confirms similar peaks at 2.69, 2.50, 1.86, 1.02, 0.61, 0.25 and 0.1 Ga, and troughs at 2.27, 1.55–1.28, 0.88–0.73, 0.38 and 0.20 Ga. Variations in the mean initial εHf and δ^{18}O values of detrital zircon grains in recent sediments show negative troughs and positive peaks, respectively, that correspond to times of supercontinent assembly (Cawood and Hawkesworth 2014). Both proxies are consistent with extensive crustal re-working at the time of assembly with more juvenile contributions representing times of supercontinent break-up and dispersal. Most importantly, all current major subdivisions of geological time, 2.5 Ga, 1.6 Ga, 1.0 Ga, 539 Ma, 252 Ma and 66 Ma, sit within the downslope of troughs that follow peaks in zircon abundance. Note, however, that the time between the 'Nuna' peak at 1.87 Ga and the currently defined Paleoproterozoic–Mesoproterozoic boundary, which precedes a long-lived abundance

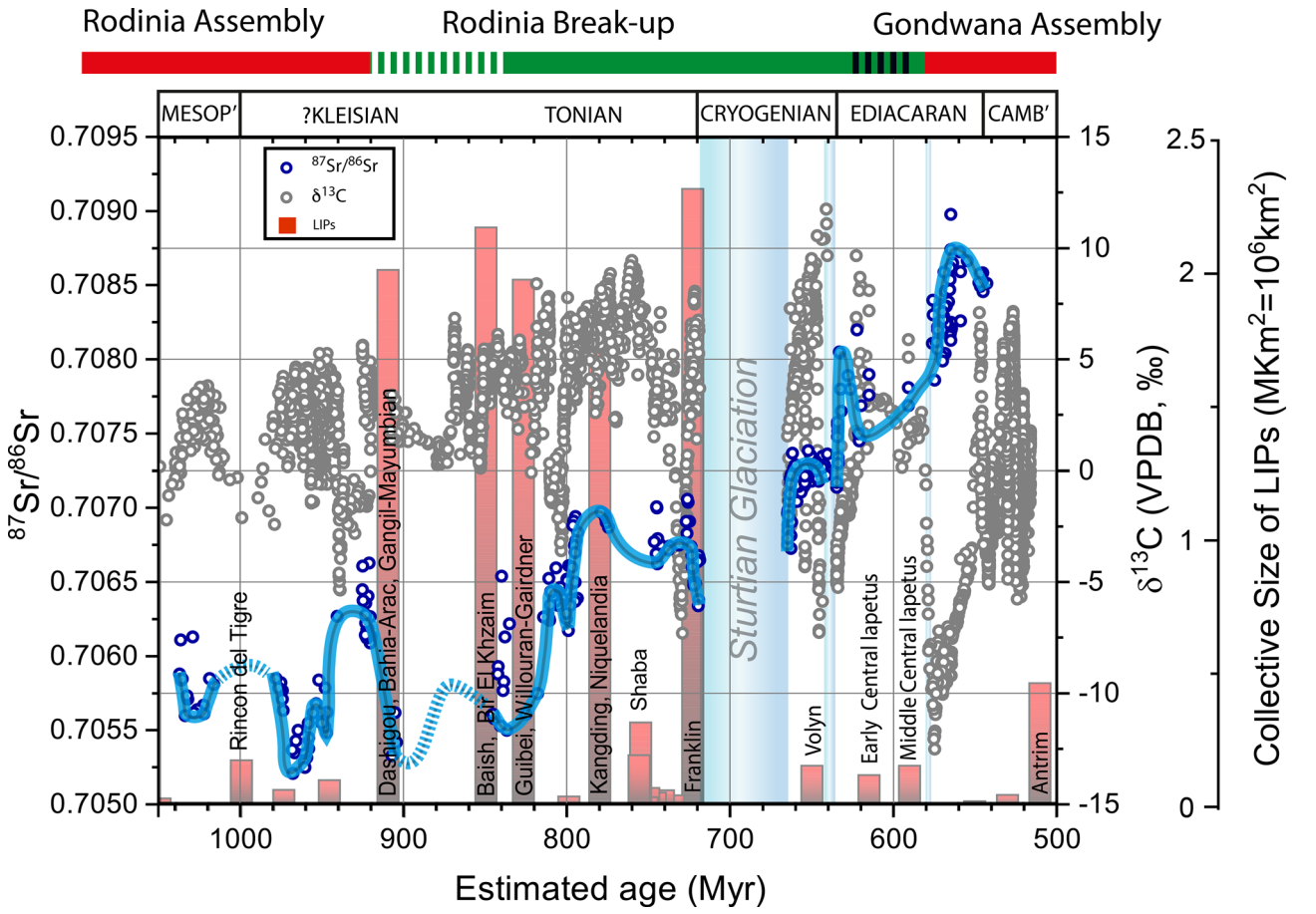

Fig. 3. A reconstructed curve of the radiogenic strontium isotope composition of Neoproterozoic seawater (blue line) superimposed on carbonate carbon isotope values (after Zhou *et al.* 2020). Seawater $^{87}Sr/^{86}Sr$ evolution reflects changes to strontium inputs to the oceans via weathering and hydrothermal exchange that are in turn linked to episodes of continental assembly and break-up (top of figure) and weathering of LIPs (red bars). Rising seawater $^{87}Sr/^{86}Sr$ through the Neoproterozoic Era can be used for global stratigraphic correlation and future chronostratigraphic subdivision.

trough, is anomalously long, and reflects protracted assembly of the Nuna supercontinent.

Strontium isotopes

The effect of crustal processes on seawater composition is recorded by the $^{87}Sr/^{86}Sr$ ratios of marine authigenic minerals, mostly carbonates. High $^{87}Sr/^{86}Sr$ values are attributed to times of increased exhumation of old, radiogenic, crystalline rocks that accompanied supercontinent amalgamation and disaggregation, while low $^{87}Sr/^{86}Sr$ values signify reduced exhumation of old crustal domains that occur during supercontinent break-up, accompanied by enhanced ocean ridge hydrothermal activity, rift-related magmatism and sea-level rise (Veizer 1989). Although commonly used seawater $^{87}Sr/^{86}Sr$ curves (Veizer 1989; Shields and Veizer 2002; Shields 2007) imply that continental weathering had little influence before the end of the Archean, recent studies (e.g. Satkoski *et al.* 2016) suggest that continental weathering of relatively radiogenic crust may have been more important than previously suspected during the Archean. Two prolonged peaks in the Sr isotope composition of seawater correspond with the Paleoproterozoic–Mesoproterozoic and Neoproterozoic–Phanerozoic transitions (Shields 2007; Kuznetsov *et al.* 2010, 2018). These intervals of enhanced continental weathering of more radiogenic rocks coincide with the amalgamation of Nuna and Gondwana, respectively (e.g. Cawood *et al.* 2013; Nance and Murphy 2018). The widespread orogenies that accompanied amalgamation of Rodinia do not feature prominently in the seawater Sr isotope curve, likely because these orogens primarily involved juvenile arcs in external orogens (e.g. Cawood *et al.* 2013; Spencer *et al.* 2013; Kuznetsov *et al.* 2017) rather than old radiogenic crustal domains. The dominant influence of lithology over weathering rates on the $^{87}Sr/^{86}Sr$ record is consistent with the observed negative covariation between the $^{87}Sr/^{86}Sr$ and detrital zircon $\varepsilon_{Hf(t)}$ records (Hawkesworth *et al.* 2016).

Strontium isotope stratigraphy is widely used as a chemostratigraphic tool (McArthur *et al.* 2020). Although the Precambrian seawater curve is still poorly constrained (Kuznetsov *et al.* 2018), the broad contours of Tonian–Cryogenian seawater $^{87}Sr/^{86}Sr$ trends are now well established (Zhou *et al.* 2020), dominated by a long-term rise in $^{87}Sr/^{86}Sr$ (from *c.* 0.7052 to 0.7073; Fig. 3). However, strontium isotope chemostratigraphy in the Neoproterozoic (and earlier) is severely limited by the small number of stratigraphic intervals containing limestones that are sufficiently well preserved (i.e. with high Sr/Ca and low Rb/Sr) to record reliably the $^{87}Sr/^{86}Sr$ of contemporaneous seawater. Therefore, the record is constructed typically from small numbers of data points from discrete intervals in different successions. When combined with limited age control on most samples, the result is an irregular record with a large number of temporal gaps and limited verification of trends among coeval successions (Fig. 3). Moreover, due to the near absence of syn-glacial carbonate strata, no proxy data for seawater exist for the Cryogenian glacial intervals (i.e. *c.* 717–660 and *c.* ≥640–635.5 Ma). Nevertheless, due to the prominent rise in $^{87}Sr/^{86}Sr$ through the Neoproterozoic (Fig. 3), the strontium isotopic record can potentially distinguish between the early Tonian (i.e. *c.* >820 Ma), late Tonian (*c.* 820–720 Ma) and Cryogenian non-glacial intervals (*c.* 660–650 Ma).

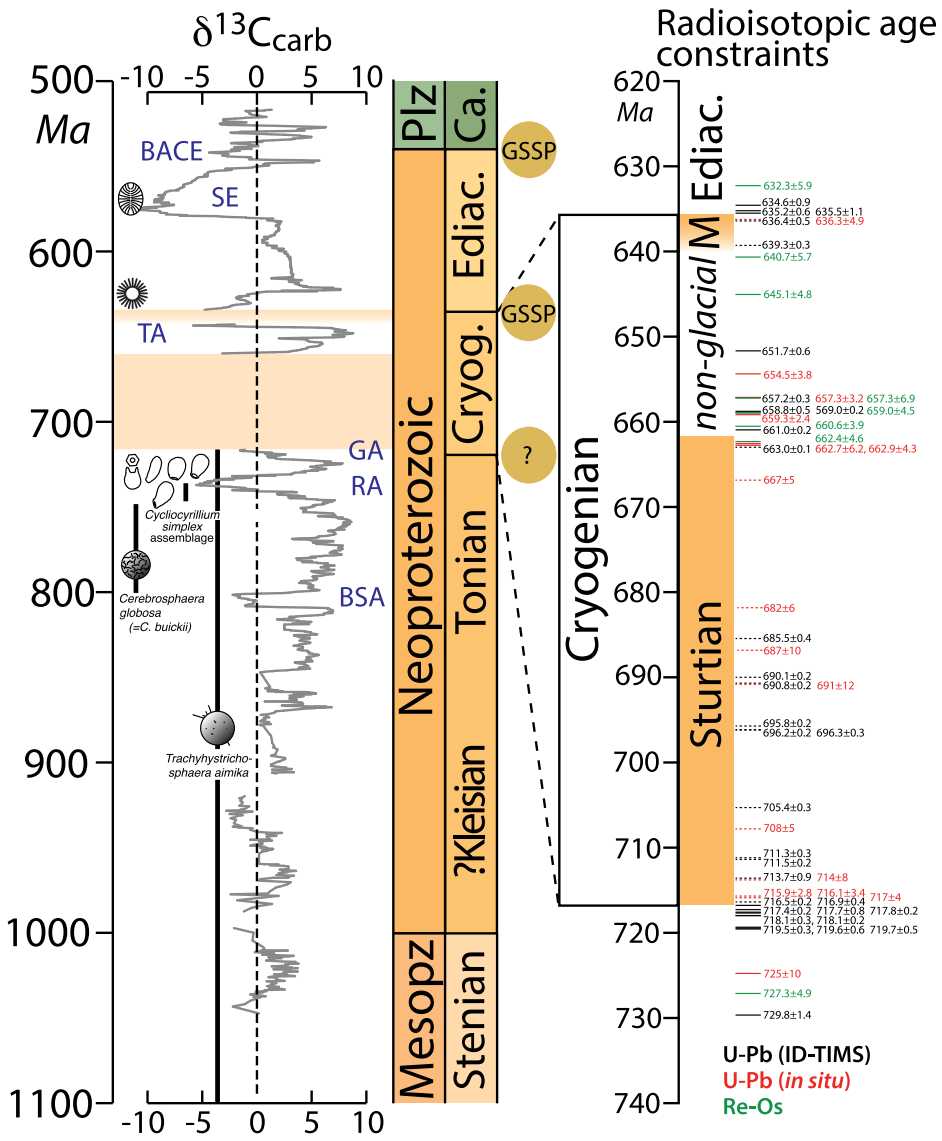

Fig. 4. The Neoproterozoic geological timescale (after Halverson *et al.* 2020). Negative carbon isotope anomalies/excursions provide useful chronostratigraphic references for subdivisions of the Neoproterozoic timescale: BSA, Bitter Springs Anomaly; RA, Russøya anomaly; GA, Garvellach anomaly; TA, Trezona Anomaly; SE, Shuram Excursion; BACE, Basal Cambrian Carbon Isotope Excursion. Minimum biostratigraphic ranges are also shown for *Trachyhystrichosphaera aimika*, *Cerebrosphaera globosa* (*C. buickii*), and the *Cycliocyrillium simplex* assemblage. Available absolute age constraints spanning the Cryogenian have multiplied in recent years and provide globally consistent estimates for the ages of the onset and end of the Sturtian and Marinoan glaciations. Here we show directly or closely stratigraphic radiometric age constraints using three approaches (volcanic zircon or baddeleyite U–Pb ages determined by isotope dilution thermal ionization mass spectrometry [ID-TIMS]; *in-situ* U–Pb ages determined by secondary ion mass-spectrometry [SIMS], sensitive high-resolution ion-microprobe [SHRIMP] or laser-ablation indicatively coupled plasma mass-spectrometry [LA-ICPMS]); and sedimentary Re-Os ages determined using ID-TIMS. Dashed lines indicate synglacial ages. Age compilation is modified from Halverson *et al.* (2020); Rooney *et al.* (2020) and Nelson *et al.* (2020).

Carbon isotopes

The carbon isotope record, mainly derived from marine carbonates, has considerable potential for subdivision of the Proterozoic geological record despite the absence of skeletal calcite (Cramer and Jarvis 2020). A widespread positive anomaly is referred to the Lomagundi-Jatuli carbon isotope excursion (LJE), which started before *c.* 2.22 Ga and ended by 2.06 Ga (Karhu and Holland 1996; Melezhik *et al.* 2007; Martin *et al.* 2013; Bekker 2014). Later negative carbon isotope anomalies in carbonate and organic carbon records have been reported at about 2.0 Ga (Kump *et al.* 2011; Ouyang *et al.* 2020), 1.6 Ga (K. Zhang *et al.* 2018; Kunzmann *et al.* 2019) and 0.93 Ga (Park *et al.* 2016), however whether they have local or global extent is not yet established. In contrast, globally correlative, high-amplitude, carbon isotope excursions are commonplace throughout the ensuing late Tonian, Cryogenian, Ediacaran and early Cambrian times (Shields *et al.* 2019).

The early Neoproterozoic carbon isotope record is identified by its sustained intervals of high $\delta^{13}C_{carb} \geq +5‰$ (Fig. 4; Kaufman *et al.* 1997; Halverson *et al.* 2005). The shift towards the high $\delta^{13}C_{carb}$ values appears to be transitional, with moderate fluctuations (≤4‰) in $\delta^{13}C_{carb}$ beginning in the late Mesoproterozoic (Knoll *et al.* 1995; Bartley *et al.* 2001; Kah *et al.* 2012) and continuing into the early Neoproterozoic (Kuznetsov *et al.* 2006). However, due to a paucity of earliest Neoproterozoic marine carbonate successions globally and poor age control on those successions that do exist, the $\delta^{13}C_{carb}$ record for the interval *c.* 1100–850 Ma is still poorly constrained (Kuznetsov *et al.* 2017). Available data indicate that significant $\delta^{13}C_{carb}$ excursions could have taken place during this interval, but values remained between −5‰ and 5‰ (Fig. 4), while $^{87}Sr/^{86}Sr$ fluctuated between 0.7052 and 0.7063 (Fig. 3; Cox *et al.* 2016; Kuznetsov *et al.* 2017; Gibson *et al.* 2019; Zhou *et al.* 2020).

The shift towards higher sustained $\delta^{13}C_{carb}$ (≥5‰) values is recorded in the Little Dal Group and equivalent strata of northwestern Canada (Fig. 4; Halverson 2006; Macdonald *et al.* 2012; Thomson *et al.* 2015). However, this trend to high $\delta^{13}C_{carb}$ values is punctuated by a discrete interval of near zero to negative $\delta^{13}C_{carb}$ values, referred to as the Bitter Springs Anomaly (BSA) (Fig. 4; Halverson *et al.* 2005) after the Bitter Springs Formation in the Amadeus Basin of central Australia where it was first reported (Hill and Walter 2000). The BSA is well documented in central Australia, Svalbard, northwestern Canada, Ethiopia (Swanson-Hysell *et al.* 2012, 2015; and references therein) and possibly India (George *et al.* 2018). It is constrained by U–Pb zircon CA-TIMS ages to have initiated after 811.5 Ma (Macdonald *et al.* 2010) and terminated prior to 788.7 Ma (MacLennan *et al.* 2018). Using a thermal subsidence-type age model applied to the Svalbard stratigraphic record, Halverson *et al.* (2018) estimated the BSA to

have begun *c.* 810 Ma and ended *c.* 802 Ma, for a duration of 8 million years.

Large Igneous Provinces (LIPs)

Plume-generated LIP magmatism could help to define natural Precambrian (and Phanerozoic) boundaries through their likely effects on the surface environments (Horton 2015; Ernst and Youbi 2017; Ernst *et al.* 2020). Examples include the Archean–Proterozoic boundary LIPs (2460–2450 Ma Matachewan and coeval events in Karelia-Kola and Pilbara cratons), Rhyacian–Orosirian LIPs (2058 Ma Bushveld and Kevitsa events), Orosirian–Statherian (1790 Ma LIPs on many cratons), Statherian–Calymmian (1590 Ma LIPs), Calymmian–Ectasian (1385 Ma LIPs on many cratons), Ectasian–Stenian (*c.* 1270 Mackenzie and 1205 Ma Marnda Moorn LIPs), Stenian–Tonian (*c.* 1005 Ma Sette Daban event or *c.* 925 Ma Dashigou event) and Tonian–Cryogenian (720 Ma Franklin LIP and other related LIPs (Ernst and Youbi 2017). Despite the difficulty of matching the isotopic record with LIP emplacement and weathering, the *c.* 720 Ma Tonian–Cryogenian boundary, now defined by the start of the Sturtian glaciation, has been linked to the Franklin LIP of northern Laurentia (Fig. 3; Macdonald *et al.* 2010; Cox *et al.* 2016; Ernst and Youbi 2017; Macdonald and Wordsworth 2017) and other LIP fragments (Ernst *et al.* 2020), potentially through enhanced weathering due to increased runoff during continental break-up and the related tropical emplacement of more easily weathered Ca- and Mg-rich flood basalts (Donnadieu *et al.* 2004). This suggestion builds on the recognition that LIPs are coeval with many Phanerozoic chronostratigraphic boundaries and that, although regional in scale, LIPs can have global environmental effects and leave a recognizable signature in global sedimentary records. Thus, while LIPs are not 'golden spikes' in themselves, they can represent proxies for golden spikes in the sedimentary record (Ernst *et al.* 2020), which bodes well for Proterozoic stratigraphic correlation along Phanerozoic lines.

Palaeontological constraints

Early attempts at biostratigraphy used distinctive forms and textures of stromatolites, which were once thought to be age-diagnostic microbialites (Riding 2011). However, evident trends are now more frequently interpreted to reflect changing environments and a general tendency towards greater biological control over calcium carbonate precipitation through time (Grotzinger 1990; Arp *et al.* 2001; Riding 2008). Few, if any, sharp temporal divisions can be identified globally in stromatolite type or microbially induced sedimentary structures (MISS). Therefore, supposedly age-diagnostic sedimentary textures, like stromatolite fabrics, have lost favour among Precambrian biostratigraphers as body fossil records have gained in popularity and abundance. Although simple leiospheres and other microscopic organic remains are known from Archean sedimentary rocks (Javaux *et al.* 2010), the oldest biostratigraphically significant fossils are macroscopic organic-walled forms known from Paleoproterozoic rocks (Han and Runnegar 1992; Javaux and Lepot 2018), now dated to *c.* 1870 Ma (Fralick *et al.* 2002; Schneider *et al.* 2002; Pietrzak-Renaud and Davis 2014). These simple coils and spirals, similar in appearance to *Grypania spiralis* (e.g. Walter *et al.* 1976; Sharma and Shukla 2009), are not diagnostically eukaryotic in affinity. Decimetre-sized seaweed-like compressions (Zhu *et al.* 2016) and ornamented acritarchs occur in rocks as old as *c.* 1.6 Ga (e.g. Miao *et al.* 2019) and are widely considered to be the first convincing fossilized eukaryotes (Javaux and Lepot 2018).

Molecular clock analyses place the origin of crown-group eukaryotes sometime in the Mesoproterozoic or late Paleoproterozoic (e.g. Berney and Pawlowski 2006; Parfrey *et al.* 2011; Eme *et al.* 2014; Betts *et al.* 2018). Some phylogenetic data suggest that the first photosynthetic eukaryotes may have emerged in freshwater habitats (Blank 2013; Sánchez-Baracaldo *et al.* 2017), which may lower their preservation potential in the rock record. The Stenian–Tonian transition interval is increasingly being viewed as a time of crown-group eukaryote diversification (e.g. Knoll *et al.* 2006*a*, *b*; Butterfield 2015; Cohen and Macdonald 2015; Xiao and Tang 2018). Latest Mesoproterozoic and earliest Neoproterozoic rocks are the first to preserve fossils with clear similarities to particular modern eukaryotic clades, including red and green algae, fungi, amoebozoans and stramenopiles (Butterfield *et al.* 1994; Porter *et al.* 2003; Butterfield 2004; Nagovitsin 2009; Loron and Moczydłowska 2017; Loron *et al.* 2019*a*, *b*; Tang *et al.* 2020), though the taxonomic affinities of most early Neoproterozoic fossils remain enigmatic. A number of eukaryotic innovations also appear in the sedimentary record during this time, including scales, tests, biomineralization and eukaryovory (Porter and Knoll 2000; Cohen and Knoll 2012; Porter 2016; Cohen *et al.* 2017*a*, *b*). In addition, eukaryote-derived sterane biomarkers appear for the first time around 810 Ma (Brocks 2018; Zumberge *et al.* 2020).

Given these evolutionary innovations, it is not surprising that late Mesoproterozoic/early Neoproterozoic fossil assemblages are largely distinct from those of early Mesoproterozoic age (Sergeev *et al.* 2017), and that several organic-walled microfossils have been proposed as index fossils for this interval. These include the acritarch *Trachyhystrichosphaera aimika* (spheroidal vesicles with sparse, irregularly distributed, hollow processes), which is found in more than 20 sections worldwide in Stenian and Tonian strata, aged *c.* 1150–720 Ma (Butterfield *et al.* 1994; Tang *et al.* 2013; Riedman and Sadler 2018; Pang *et al.* 2020) and *Cerebrosphaera globosa* (=*C. buickii*), robust spheroidal vesicles with distinctive wrinkles, common in late Tonian units *c.* 800–740 Ma (Hill and Walter 2000; Grey *et al.* 2011; Riedman and Sadler 2018; Cornet *et al.* 2019) (Fig. 4).

Several other distinctive fossils from *c.* 780–740 Ma sedimentary rocks have potential for subdividing the Tonian, but there are too few occurrences known at present to have confidence in their ranges (Riedman and Sadler 2018). Many long-ranging early Neoproterozoic and late Mesoproterozoic taxa may be biostratigraphically useful with respect to their last appearances, and in this regard it is worth noting that Riedman and Sadler (2018) found that the disappearance of many ornamented taxa in the late Tonian occurred just before or around the time when distinctive vase-shaped microfossils appear. The vase-shaped microfossils, constrained to the time from *c.* 790–730 Ma (Riedman and Sadler 2018; Riedman *et al.* 2018), provide the most promising biostratigraphic marker for subdividing Tonian time and might be useful in defining the Cryogenian GSSP (Strauss *et al.* 2014), although the extent to which the stratigraphic range is controlled by taphonomic factors is not yet clear.

Reassessment of the pre-Cryogenian timescale and recommendations for future development

The embryonic nature of Proterozoic bio- and chemostratigraphy outlined above illustrates that ratification of pre-Cryogenian GSSPs lies far in the future and beyond the scope of the current review, which is focussed on a template for agreed rock-based criteria to permit the removal of current GSSAs and their replacement with interim chronostratigraphic units, bounded by approximate ages. Development of a natural Precambrian timescale, especially for periods (systems), is still a 'work in progress', but we consider nevertheless that improved rock-based subdivision is already possible, desirable and overdue. In working towards this aim, it is important not to overlook the merits of the established chronometric scheme, which has served geologists well over the last 30 years.

Indeed, it would appear that most boundaries would change by only small degrees. In order for future units of time (and strata) to be both widely acceptable and scientifically meaningful, they need to be fully defined conceptually, as has been done for the Cryogenian, Ediacaran and Cambrian periods, before they can be pinned down numerically.

There is general agreement that the boundary definitions for the Hadean, Archean, Proterozoic and Phanerozoic eons help to broadly delimit four distinct parts of Earth history that are characterized by particular tectonic and biogeochemical regimes. Similarly, the eras of the Proterozoic Eon are recognized to be distinct intervals of tectonic, environmental and biological significance. The goal of any revision of the Precambrian geological timescale should therefore be to minimize disruption to both the current international timescale and existing regional and national stratigraphic norms. In this vein, it is pertinent to recall the advice given by James (1978, p. 200), following Trendall (1966), that:

> (1) the classification should be the simplest possible that will meet immediate needs [as] every additional complexity provides a basis for disagreement or rejection; (2) The subdivision of time embodied in the classification should reflect major events in Earth's history, yet not be in such a form as to inhibit critical review of that history; (3) The classification must be acceptable to most students of the Precambrian; (4) The nomenclature should not be identified closely with one particular region; and (5) The subdivision scheme should be accompanied by operational criteria, so that assignment to the classification will be guided by objective rather than theoretical considerations.

It is in this spirit that we explore below how an improved rock-based geological timescale might depart from the existing chronometric timescale.

Archean Eon (*c.* 4.0 to 2.45 Ga)

The Archean Eon witnessed early crustal formation and thickening, leading to the formation and emergence of the first cratons and platform sedimentation. It is characterized by granite-greenstone terranes and the extrusion of ultramafic lavas (komatiites), which are extremely uncommon in post-Archean rocks (Arndt 2008; Sossi *et al.* 2016). Apart from the recognized granite-greenstone terranes and younger platform covers, the Archean is characterized by high-grade, polymetamorphic granite-gneiss complexes.

Subdivision of the chronometric Archean Eon is not formalized (Plumb 1991). Nevertheless, the Subcommission on Precambrian Stratigraphy (SPS) voted in 1991 and 1995 to pursue formal subdivision into four eras: Eoarchean (>3.6 Ga), Paleoarchean (3.6 to 3.2 Ga), Mesoarchean (3.2 to 2.8 Ga), and Neoarchean (2.8 to 2.5 Ga) (Fig. 1a); no reasons for the choice of these boundaries were given. Since these subdivisions have not been formally ratified (Robb *et al.* 2004), they are considered to be recommendations only (Bleeker 2004*a*). An alternative tripartite chronostratigraphic scheme was proposed by Van Kranendonk *et al.* (2012): the Paleoarchean (4.03 to 3.49 Ga), Mesoarchean (3.49 to 2.78 Ga) and Neoarchean (2.78 to 2.42 Ga); each composed of a number of periods (Fig. 1b). The base of the Paleoarchean in the 2012 proposal was defined by the age of the oldest extant rocks, the Acasta Gneiss in Canada, while the base of the overlying Mesoarchean was defined at the oldest microbially-influenced textures in stromatolites of the North Pole Dome in western Australia (Van Kranendonk *et al.* 2003; Allwood *et al.* 2007), thus representing the oldest potential 'golden spike' (Fig. 1b). The Paleoarchean contained an 'Acastan Period', the lower limit of which was defined by the oldest preserved rocks (Acasta Gneiss, Canada; Stern and Bleeker 1998; Bowring and Williams 1999) and an 'Isuan Period', starting at 3.81 Ga to represent when Earth's oldest supracrustal suite in the Isua Supracrustal Belt in Greenland was deposited.

The problem with using the oldest occurrence of a particular sedimentary rock type to subdivide geological time is that it may reflect chance preservation rather than any fundamental change in geological processes, and older examples may be discovered. This is exemplified by the choice of the Isua Supracrustal Belt, which contains older metasedimentary rocks (Nutman *et al.* 1996) that might blur the distinction between the Acastan and Isuan 'periods.' It also runs counter to the concept of the international geological timescale as a correlative 'stratigraphic' framework, leading us to support leaving the base of the Archean at *c.* 4.0 Ga, pending formal definition of the Hadean–Archean boundary. A similar problem arises with the placement of the base of the Mesoarchean at *c.* 3.49 Ga for the North Pole Dome stromatolites as the occurrence of stromatolites is controlled by the particular environment, rather than representing a definable moment in evolution. A less ambiguous boundary for the base of the Mesoarchean might be the near-coeval base of the oldest, well-preserved Barberton and Pilbara supracrustal successions, although the global relevance of such a definition still needs strengthening.

Van Kranendonk *et al.* (2012) also proposed changing the end of the Archean to *c.* 2.42 Ga, based on the first widespread appearance of 'Huronian' glacial deposits in the rock record (Gumsley *et al.* 2017; Young 2019; Bekker *et al.* 2020, 2021) and the approximately contemporaneous change to an oxygenated atmosphere (Great Oxidation Episode or GOE; see Poulton *et al.* 2021 for the nuanced texture of this event), which followed the end of the world's greatest development of banded iron formation (BIF). This approach seems reasonable based on the rock record, which constrains globally significant climatic and atmospheric changes to this time (Gumsley *et al.* 2017). The GOE has been defined in various ways, but in recent years has been presumed to begin when atmospheric oxygen had accumulated to sufficient levels to prevent the formation and/or preservation of mass-independent S-isotope fractionation (MIF-S) in the lower atmosphere and sedimentary rocks, respectively (Farquhar *et al.* 2000; Bekker *et al.* 2004). However, its onset and duration are still inadequately constrained (e.g. Luo *et al.* 2016; Poulton *et al.* 2021) and it may not have been synchronous everywhere (Philippot *et al.* 2018; see for the rebuttal to this view Bekker *et al.* 2020, 2021). Our alternative view is that the end of the major phase of late Archean BIF deposition is of greater significance in the context of the present discussion. The Archean–Proterozoic boundary might therefore be best constrained/defined by accurately dated tuffs (*c.* 2.45 Ga) at the top of the Hamersley Group in Western Australia (Trendall *et al.* 2004); BIFs in the Transvaal Basin of South Africa are approximately coeval (Bekker *et al.* 2010; Lantink *et al.* 2019). This would imply redefining the Siderian Period, named for the global peak in iron formations in the sedimentary records, and moving it into the Neoarchean (cf. Van Kranendonk *et al.* 2012), thereby addressing also the criticism that a numerical boundary at 2.5 Ga splits this important acme in iron formation deposition.

Complementary records of Archean change are provided by geochemical and isotopic studies of magmatic rocks that appear to indicate major secular changes in tectonic processes (Kamber and Tomlinson 2019). On this basis, Griffin *et al.* (2014) concurred that the Archean Eon is best divided into three eras: 'Paleoarchean' (4.0–3.6 Ga), 'Mesoarchean' (3.6–3.0 Ga) and 'Neoarchean' (3.0–2.4 Ga). In this interpretation, during the 'Paleoarchean' Era, Earth's dominantly mafic crust acted as a stagnant-to-sluggish lid. Dating of zircon grains from near the close of the era reveal subtle geochemical signs of a change in tectonic regime interpreted as a transition from granitoid production from oceanic plateaus to some form of felsic magmatism in arc-like (subduction-related) settings (Ranjan *et al.* 2020). It has been suggested that the subsequent

'Mesoarchean' was dominated by major episodes of mantle overturn and plume activity (Van Kranendonk 2011) that led to development of the subcontinental lithospheric mantle and a steady increase between *c.* 3.3 and 3.0 Ga in the K_2O/Na_2O ratios of TTG (tonalite–trondhjemite–granodiorite) rock suites (Johnson *et al.* 2019). However, early evidence of subduction is also inferred at this time, along with diapiric doming, in adjoining terranes of the Pilbara Craton (Hickman 2004; Van Kranendonk *et al.* 2004). Pre-3.0 Ga fluvial sediments imply at least some early regional emergence on the Pilbara, Kaapvaal and Singhbhum cratons (Heubeck and Lowe 1994).

The Neoarchean witnessed the continued transition to some form of plate tectonics, and the development of significant volumes of more felsic continental crust, characterized by the first K-rich granitoids (Bédard 2018; Cawood *et al.* 2018). However, gravity-driven doming and plume activity was still an active process in the formation of granite-greenstone terranes *c.* 2.72–2.60 Ga (Jones *et al.* 2020). Progressive cratonization is reflected in the development of the first extensive platform covers after about 3.0 Ga, e.g. the Witwatersrand and Ventersdorp supergroups, and also Pongola Group on the Kaapvaal Craton (Frimmel 2019), the Mount Bruce Supergroup on the Pilbara Craton, and in Canada the Central Slave Cover Group (Bleeker *et al.* 1999; Sircombe *et al.* 2001) and the oldest thick carbonate platform: the *c.* 2.79 Ga Steep Rock Lake Group (Riding *et al.* 2014; Fralick and Riding 2015). The first development of extensive sedimentary platforms overlying stable cratons provides a logical interim boundary within the Archean, and so the base of the Neoarchean could be placed at *c.* 3.1–2.9 Ga, which would bracket earliest evidence for widespread but transient oxygenation of the surface marine environment (Anbar *et al.* 2007; Riding *et al.* 2014; Ossa Ossa *et al.* 2019; Ostrander *et al.* 2019). Increasing lithospheric stability is also supported by the oldest extensive mafic dyke swarms between *c.* 2.8 and 2.7 Ga (Evans *et al.* 2017; Cawood *et al.* 2018; Gumsley *et al.* 2020).

It seems significant that the youngest widespread granite-greenstone terranes (e.g. Yilgarn, southern Superior craton and Bulawayan) are coeval with the basalt-rich Fortescue and Ventersdorp platform covers. We tentatively suggest that this could form a basis for future subdivision of the Neoarchean, potentially into three periods based on the rock records of a newly defined Siderian Period (see above), the coeval Fortescue–Ventersdorp groups and the Witwatersrand-Pongola groups, respectively. Cratonization culminated in a globally stable 'super-craton' regime around the traditional Archean–Proterozoic boundary (Bleeker 2003; Cawood *et al.* 2018) with the oldest supercraton, Superia, nearly assembled at the proposed Archean–Proterozoic boundary. Depending on the outcome of further research on the global distribution and timing of cratonization events, the term *Kratian*, after the Greek root 'kratos' or strength, could be considered a possible name for one of these older periods.

In summary: (1) we agree with previous workers (e.g. Van Kranendonk *et al.* 2012; Griffin *et al.* 2014) that the current chronometric subdivision of the Archean should be modified from four to three rock-based eras by discontinuing use of the Eoarchean as an era-level subdivision, (2) we suggest that the three remaining eras could be of approximately equal duration, comprising the Paleoarchean (*c.* 4.0–3.5 Ga), the Mesoarchean (*c.* 3.5–3.0 Ga) and the Neoarchean (*c.* 3.0–2.45 Ga) and (3) we concur that the Siderian should be moved to the terminal Neoarchean (Van Kranendonk *et al.* 2012) and propose that it ends at *c.* 2.45 Ga (Fig. 1c).

Proterozoic Eon (*c.* 2.45 to 0.54 Ga)

The base of the Proterozoic Eon broadly corresponds to the change to an Earth that had developed some aspects of modern plate tectonics and was increasingly characterized by stabilized, emergent continental (super)cratons. The chronometric base of the Proterozoic Eon precedes quite closely widespread evidence for glaciation, the GOE and a change from wholly anoxic oceans to a more complex ocean redox structure characterized by variously oxic, anoxic-ferruginous and anoxic-euxinic portions (Poulton *et al.* 2021). Consequently, the boundary must represent a planetary step change that significantly transformed Earth's biogeochemical cycles, presumably accompanied by the development of novel microbial pathways and metabolisms, leading eventually to larger and more complex (eukaryotic) forms. The Proterozoic marine sedimentary rock record is also marked by a greater diversity of authigenic minerals (Hazen 2010; Hazen *et al.* 2011) and carbonate textures (James *et al.* 1998; Shields 2002; Hodgskiss *et al.* 2018).

Paleoproterozoic Era (c. 2.45 to 1.8 Ga)

The Paleoproterozoic Era witnessed the transition from an Archean tectonic regime of scattered, small cratons to a more conventional form of plate tectonics (Bleeker 2003; Liu *et al.* 2021). Tectonic collisions subsequently resulted in formation of Earth's earliest widely accepted supercontinent, Nuna or Columbia (Hoffman 1989, 1997; Rogers and Santosh 2002; Zhao *et al.* 2002; Bleeker 2003; Payne *et al.* 2009; Evans and Mitchell 2011; Zhang *et al.* 2012; Mitchell 2014; Yang *et al.* 2019; Kirscher *et al.* 2021), as evidenced by *c.* 2.0–1.6 Ga orogenic belts on all present-day continents and widespread seismically imaged dipping structures indicating a global subduction network by this time (Wan *et al.* 2020). Reassigning the Siderian to the Neoarchean requires a new period to be defined and named for the earliest Paleoproterozoic. Van Kranendonk *et al.* (2012) refer to this period as the Oxygenian Period, although we consider *Skourian*, after the Greek word for rust, to be a suitable, rock-based alternative (Fig. 1c).

The Paleoproterozoic sedimentary record provides clues to significant events, some of which are likely to have been global in scale and can probably be related to the large-scale tectonic processes outlined above. Abundances of molybdenum, uranium, selenium, sulfate and iodate increased in marine sedimentary rocks in multiple Paleoproterozoic basins, indicating growth in ocean reservoirs of those redox-sensitive species (Scott *et al.* 2008; Partin *et al.* 2013; Hardisty *et al.* 2017; Kipp *et al.* 2017; Blättler *et al.* 2018). This trend has been interpreted as evidence of oxidative weathering caused by atmospheric oxygenation during and after the GOE together with expansion of oxic conditions in the marine realm, which stabilized these elements as oxyanions in solution, while titrating redox-sensitive iron, manganese and cerium out of solution by oxidation (Tsikos *et al.* 2010; Warke *et al.* 2020*a*). Accumulation of iron formations (IFs) peaked around the Archean–Proterozoic boundary, but episodically continued until *c.* 1.8 Ga (Klein 2005), after which major BIF deposits are scarce, but not entirely absent (Bekker *et al.* 2010, 2014; Canfield *et al.* 2018). Initially, the decline in the abundance of BIF was attributed to the widespread development of euxinic waters on productive continental shelves at *c.* 1.84 Ga, which titrated ferrous iron in the form of pyrite (Canfield 1998; Poulton *et al.* 2010; Poulton and Canfield 2011). However, ferruginous deeper oceans persisted throughout most of the mid-Proterozoic (Poulton *et al.* 2010), and the paucity of BIF through this period is likely also related to diminished hydrothermal sources of iron after *c.* 1.8 Ga (Cawood and Hawkesworth 2014). The disappearance of redox-sensitive detrital minerals, such as pyrite, uraninite and siderite, has long been attributed to the GOE (Holland 1984, 2006; Frimmel 2005; Van Kranendonk *et al.* 2012), the onset of which is generally considered to have been approximately contemporaneous with what some have interpreted as the Earth's first global-scale glaciations (Bekker and Kaufman 2007; Brasier *et al.* 2013; Tang and Chen 2013; Bekker 2014; Young 2019; Bekker *et al.* 2020). The strongest evidence for

a Paleoproterozoic Snowball Earth comes from South Africa, with palaeomagnetic evidence of low-latitude glaciation in the Makganyene Formation at *c.* 2.43 Ga (Evans *et al.* 1997; Gumsley *et al.* 2017). This glaciation is considered to have occurred shortly after the initial disappearance of MIF-S isotope fractionation, as recorded in pre-glacial sediments in Karelia (Warke *et al.* 2020*b*; see also Bekker *et al.* 2020).

Paleoproterozoic glacial episodes were followed by the Earth's largest known positive $\delta^{13}C$ excursion(s), the LJE, between *c.* 2.31–2.22 and *c.* 2.11–2.06 Ga (Martin *et al.* 2013, 2015), which accompanied the first major evaporitic sulfate deposits (Melezhik *et al.* 2005; Schroder *et al.* 2008; Brasier *et al.* 2011; Blättler *et al.* 2018) and permanent atmospheric oxygenation (Poulton *et al.* 2021). The LJE was in turn followed by the *c.* 2.06 Ga Shunga Event that is characterized by a major accumulation of C_{org}- and pyrite-rich sedimentary rocks and the generation of giant petroleum deposits (Melezhik *et al.* 2004) as well as the first sedimentary phosphorite deposits (Kipp *et al.* 2020). The Shunga Event interestingly coincides with the emplacement of the Bushveld (Kaapvaal Craton) and the Kevitsa (Karelia Craton) LIPs (e.g. Ernst *et al.* 2020), which inspired the name of the chronometric Rhyacian Period (2.3–2.05 Ga) after the Greek word *rhyax* (meaning streams of lava; Plumb 1991). One potentially distinctive feature of the middle Paleoproterozoic is a disputed tectono-magmatic lull between *c.* 2.3 and 2.2 Ga (Spencer *et al.* 2018), during which evidence for juvenile magmatism and orogenesis is scarce, but not entirely absent (Partin *et al.* 2014; Moreira *et al.* 2018). Juvenile magmatism reinitiated after *c.* 2.2 Ga (Condie *et al.* 2009; Spencer *et al.* 2018) as well as episodic rifting, which eventually succeeded in the break-up of the Superia supercraton. The chronometric Rhyacian–Orosirian boundary (2050 Ma) possibly correlates also with an abrupt increase in magnitude of a mass-independent O-isotope anomaly of photochemical origin that is carried in sedimentary sulfate minerals (gypsum/anhydrite and barite). The observed step-like secular shift to a large (negative) $\Delta^{17}O$ anomaly is tentatively ascribed to a collapse without parallel in global gross primary productivity (Crockford *et al.* 2019; Hodgskiss *et al.* 2019) and the ushering in of a period of more muted isotopic variability and low oxygen levels.

The first macroscopic organic-walled fossils, coiled forms similar to *Grypania spiralis*, appear within the Orosirian strata by *c.* 1.89 Ga (Han and Runnegar 1992; Javaux and Lepot 2018) to be joined by large, more convincingly eukaryote-grade fossils by the end of the era (Zhu *et al.* 2016; Miao *et al.* 2019). The Paleoproterozoic fossil record contains the *c.* 1.89 Ga Gunflint fossil microbes, which are taken to be the oldest unambiguous evidence of either iron-oxidizing bacteria or oxygenic cyanobacteria (Planavsky *et al.* 2009; Crosby *et al.* 2014; Lepot *et al.* 2017), although older cyanobacterial fossils are known also from the *c.* 2.0 Ga Belcher Group in eastern Hudson Bay (Hofmann 1975; Hodgskiss *et al.* 2019).

A period of worldwide orogeny and major crustal growth occurred during the Orosirian Period from *c.* 2.25 to 1.78 Ga and is reflected in an exceptional zircon abundance peak (Fig. 2). This peak reaches its acme between 1.90 and 1.85 Ga (Condie 1998, 2004; Puetz and Condie 2019; Condie and Puetz 2019) and is interpreted to correspond to the formation of the supercontinent Nuna. Nuna assembly started with *c.* 2.25–2.0 Ga collisional orogenies in Amazonia, São Francisco, West Africa, Sarmatia and Volgo-Uralia (Shumlyanskyy *et al.* 2021). The Laurentia portion of Nuna largely assembled between *c.* 2.0 and 1.8 Ga, with the Rae Craton serving as the upper plate (Hoffman 2014), starting with the *c.* 1970 Ma Thelon orogeny (Bowring and Grotzinger 1992). Accretionary orogenies continued through the Statherian, with the *c.* 1.6–1.4 Ga final suturing events extending into the Calymmian in Australia on the periphery of Nuna (Pourteau *et al.* 2018; Kirscher *et al.* 2019, 2021; Yang *et al.* 2019; Gibson *et al.* 2020). The protracted record of collisional orogenesis between *c.* 2.0 and *c.* 1.4 Ga has historically led to difficulties in defining the boundary between the Paleoproterozoic and the Mesoproterozoic. Thus, the Precambrian Subcommission expressed 'individual preferences … from 1400 to 1800 Ma' and eventually settled on 1600 Ma (Fig. 1a; Plumb and James 1986).

The Statherian Period (*c.* 1.8–1.6 Ga) is currently defined as marking the end of the Paleoproterozoic Era (Fig. 1a). It is characterized by the widespread development of shallow-marine, intracratonic, unmetamorphosed, sedimentary basins with expansive carbonate deposits covering increasingly stable cratons following Nuna amalgamation. However, the defining characteristics of the Statherian Period are remarkably similar to those of the ensuing Calymmian Period (see below), which represents the oldest segment of the Mesoproterozoic Era as currently defined (Fig. 1a). A number of Statherian successions, such as the *c.* 1.7–1.4 Ga Changcheng-Jixian groups of the Sino-Korean or North China Craton, are traditionally considered and mapped as Mesoproterozoic successions (Zhao and Cawood 2012), despite their deposition prior to 1.6 Ga. Other classic, mid-Proterozoic, but pre-1.6 Ga units originally envisaged to fall within the chronometric Proterozoic II (Plumb and James 1986) include the Tawallah and McArthur groups of northern Australia (Rawlings 1999); the lower Riphean Burzyan Group of the Urals, Russia (Puchkov *et al.* 2014; Semikhatov *et al.* 2015); the Espinhaço Supergroup and Araí Group of Brazil and coeval Chela Group of central Africa Chemale *et al.* 2012; Guadagnin *et al.* 2015); the Vindhyan and Cuddupah supergroups of India (Ray 2006; Collins *et al.* 2015; Chakraborty *et al.* 2020) and the Uncompahgre Group of SW Colorado, USA, which was deposited during the late stages of the 1.71–1.68 Ga Yavapai Orogeny (Whitmeyer and Karlstrom 2007).

Given a better understanding of the nature and timing of Nuna assembly and continuing difficulties in differentiating between the defining characteristics of the Statherian and Calymmian periods, we recommend that the end of the Paleoproterozoic be provisionally redefined at *c.* 1.8 Ga, with the Statherian placed in the Mesoproterozoic (Puchkov *et al.* 2014), pending future definition of GSSPs. This age follows latest Orosirian orogeny and magmatism, and precedes the onset of widespread platform cover after about 1.8 Ga. Redefinition of the end of the Paleoproterozoic to *c.* 1.8 Ga also has the merit of linking it more closely to the detrital zircon record (Fig. 2).

Mesoproterozoic Era (c. 1.8 to 1.0 Ga)

The Mesoproterozoic Era represents a period of seeming overall stability in Earth history, during which were long thought to be few changes in the sedimentary record, biogeochemical cycling, climate and biological evolution (Buick *et al.* 1995; Brasier and Lindsay 1998), making it particularly difficult to subdivide. As summarized by Cawood and Hawkesworth (2014), the period from 1.7 to 0.75 Ga is characterized by a paucity of passive margins (Bradley 2008), anoxic-ferruginous and regionally euxinic marine environments (Poulton *et al.* 2004, 2010), an absence of significant Sr isotope variations in the seawater record (Shields 2007; Kuznetsov *et al.* 2017), few highly evolved $\varepsilon_{Hf(t)}$ values in zircon grains, limited orogenic gold and volcanogenic massive sulphide ore (but major sedimentary exhalative Pb-Zn) deposits, an absence of glacial deposits and a paucity of massive iron formations. However, significant developments include formation of the oldest economical phosphorite deposits at *c.* 1.6 Ga in India and Australia (McKenzie *et al.* 2013; Crosby *et al.* 2014; Chakraborty *et al.* 2020; Fareeduddin and Banerjee 2020) and the emplacement of *c.* 1.5–1.2 Ga massif anorthosites and related intrusive rocks (Whitmeyer and Karlstrom 2007; McLelland *et al.* 2010; Ashwal and Bybee

2017). The development of massif anorthosite at this point was attributed by Cawood and Hawkesworth (2014) to secular cooling of the mantle to a temperature at which continental lithosphere was strong enough to be thickened, but still warm enough to result in melting of the lower thickened crust.

As currently defined, the early Mesoproterozoic Calymmian Period (*c.* 1.6–1.4 Ga) and the middle Mesoproterozoic Ectasian Period (*c.* 1.4–1.2 Ga) are both characterized by the progressive development of new platform cover successions (Fig. 1a). In northern Australia, the base of the Calymmian System is represented by an unconformity that separates the overlying Nathan Group from the underlying (Statherian) McArthur Group (Rawlings 1999). Thick terrigenous basins that developed during the Calymmian Period following the final amalgamation of Nuna include the Roper Group, North Australia (Rawlings 1999), Belt-Purcell supergroups, North America (Ross and Villeneuve 2003), Paraguaçu–Chapada Diamantina groups, Brazil (Guadagnin *et al.* 2015) and the Changcheng and Jixian groups, China (Qu *et al.* 2014). Microbially influenced carbonates of the Jixian Group could provide a suitable Calymmian 'stratotype'. Deposition of the upper Roper Group in Australia, Xiamaling Formation in North China (Meng *et al.* 2011), Yurmatau Group in Urals, Russia (Semikhatov *et al* 2015) and the Kibara Supergroup and equivalents in central Africa (Fernandez-Alonso *et al.* 2012) during the Ectasian accompanied the break-up of the core of supercontinent Nuna (Evans and Mitchell 2011; Pisarevsky *et al.* 2014).

Although there is currently little to distinguish the Calymmian and Ectasian periods, they are retained as separate entities in Figure 1c. Potential rock-based markers for the Calymmian–Ectasian boundary are elusive. Regional-scale, magmatic events such as the *c.* 1.32 and 1.23 Ga dyke/sill swarms of North China (Peng 2015; Zhai *et al.* 2015; Wang *et al.* 2016; Zhang *et al.* 2017), the 1.32 Ga swarm of northern Australia (Yang *et al.* 2020; Bodorkos *et al.* 2021), the *c.* 1.27 Ga Mackenzie dyke swarm in Canada and the *c.* 1.12–1.08 Ga Ghanzi-Chobe-Umkondo and Midcontinent Rift systems have not been linked to any global-scale isotopic excursions that could be used for correlation. However, the coincidence of widespread *c.* 1385 Ma LIPs and black shales has been proposed as a potential rock-based marker for the Calymmian–Ectasian boundary (S.H. Zhang *et al.* 2018. The C-isotope record is relatively monotonous although some structure is emerging (e.g. K. Zhang *et al.* 2018; Shang *et al.* 2019).

Increasingly convincing discoveries of fossil eukaryotes, in the form of large, multicellular, organic-walled fossil fronds and ornamented acritarchs (Zhu *et al.* 2016; Miao *et al.* 2019) first occur in rocks that straddle the current chronometric Paleoproterozoic–Mesoproterozoic boundary, indicating high potential for further Mesoproterozoic fossil discoveries. Current fossil and molecular evidence agree that crown group Archaeplastida (a group that includes the red, green and glaucophyte algae) emerged during the Mesoproterozoic Era (Butterfield 2000; Eme *et al.* 2014), or possibly even earlier in non-marine environments (Sánchez-Baracaldo *et al.* 2017). Multicellular eukaryotic algae appear before 1.0 Ga in the form of isolated examples of red algae (*Bangiomorpha pubescens* at *c.* 1.05 Ga) and green algae (*Proterocladus antiquus* at *c.* 1.0 Ga) (Butterfield *et al.* 1994; Tang *et al.* 2020), with putative earlier examples of red algae from India (*Rafatazmia chitrakootensis* and *Ramathallus lobatus)* at *c.* 1.6 Ga (Bengtson *et al.* 2017). Ornamented acritarchs are more common eukaryote-grade fossils and some may prove useful for biostratigraphy. For example, *Tappania plana* is a widely reported Mesoproterozoic fossil taxon, which has been found in the Ruyang Group of China (Yin 1997; Yin *et al.* 2018), Roper Group of Australia (Javaux *et al.* 2001; Javaux and Knoll 2017), Siberia (Nagovitsin 2009), the Belt Supergroup of USA (Adam *et al.* 2017) and Singhora Group, India (Singh *et al.* 2019). Therefore, the Mesoproterozoic Era, although often given the epithet 'boring', marks the point in geological time when biostratigraphy becomes possible.

The final period of the Mesoproterozoic was named 'Stenian' with reference to what was interpreted as a worldwide network of linear orogenic belts that were grouped as 'Grenvillian' (Plumb 1991). Although the supposed continuity and contemporaneity of these belts worldwide can be challenged in detail (e.g. Fitzsimons 2000), there is broad consensus that this period of collisional orogenies led to formation of the supercontinent Rodinia by *c.* 950 Ma (Li *et al.* 1999; Evans *et al.* 2016; Merdith *et al.* 2017*a*). The type Grenvillian (NE Canada; Rivers 2015), the Sveconorwegian (Scandinavia; Bingen *et al.* 2021), the Sunsas (South America; Teixeira *et al.* 2010), the Natal-Namaqua (Africa; Cornell *et al.* 2006) and the Albany-Fraser (Australia; Spaggiari *et al.* 2015) orogenic belts all display similar records of high-grade metamorphism and magmatism between *c.* 1200 and 1000 Ma (see also Cawood and Pisarevsky 2017). Defining a chronostratigraphy on the basis of high-grade metamorphic events is problematic, but an interim arbitrary duration of *c.* 1200 to 1000 Ma (Figs 1a and c) encompasses the main orogenic events across the 'Grenvillian' belts and corresponds with a prominent spike in the detrital zircon record (Fig. 2). Additionally, the end of the period marks the appearance of multicellular red and green algae in the fossil record (Xiao and Tang 2018; Tang *et al.* 2020).

Neoproterozoic Era (c. *1.0 to 0.54 Ga)*

The Neoproterozoic Era records a number of highly significant events in Earth history (Shields 2017). New platform cover successions were deposited during the final amalgamation, tenure and break-up of Rodinia. Eukaryotes continued to diversify within an environment characterized by rising, but unstable seawater $^{87}Sr/^{86}Sr$ (Zhou *et al.* 2020), high-amplitude $\delta^{13}C$ excursions (>8‰), climate perturbations, and episodic ocean oxygenation: the 'Neoproterozoic Oxygenation Event' (Och and Shields-Zhou 2012). Following a prolonged interval of unusually widespread glaciation (Hoffman *et al.* 2017), the end of the era was marked by the evolution of the unique Ediacaran multicellular biota, and widespread orogenesis associated with the assembly of Gondwana through the late Ediacaran to early Cambrian interval.

The subdivision of Neoproterozoic time has largely been informed by (1) the occurrence and correlation of two widespread glacial units now known to be of Cryogenian age (Thomson 1871, 1877; Reusch 1891; Kulling 1934; Lee 1936; Howchin 1901; Mawson 1949) and (2) fossils of metazoan affinity that postdate those glaciogenic deposits, but predate Cambrian strata (Glaessner 1962). Harland (1964) first proposed the term 'infra-Cambrian' or 'Varangian' for a terminal Precambrian system (Fig. 5) based on two discrete diamictite units, the Smalfjord (Bigganjargga) and Mortensnes formations on the Varanger Peninsula, NE Norway, first described by Reusch (1891); Harland (1964) proposed that the start of this new period should correspond to the base of the lower of these two glacial horizons, believing them to be stratigraphic equivalents of globally widespread glaciogenic units in, for example, Greenland, Spitsbergen, Canada and Australia (Harland 1964). However, the two glacial units of the Varanger Peninsula were later found to include an Ediacaran glaciogenic unit of only regional extent (Rice *et al.* 2011), leading to abandonment of the term 'Varangian' or 'Varangerian'. Dunn *et al.* (1971) introduced the terms 'Sturtian' and 'Marinoan', named after Sturt Gorge and Marino Rocks near Adelaide in South Australia, for the two Cryogenian glacial epochs recorded there, emphasizing their utility as chronostratigraphic markers. Cloud and Glaessner (1982) proposed the term 'Ediacarian' for the interval spanning from the upper limit of these glacial deposits to the base of the Cambrian.

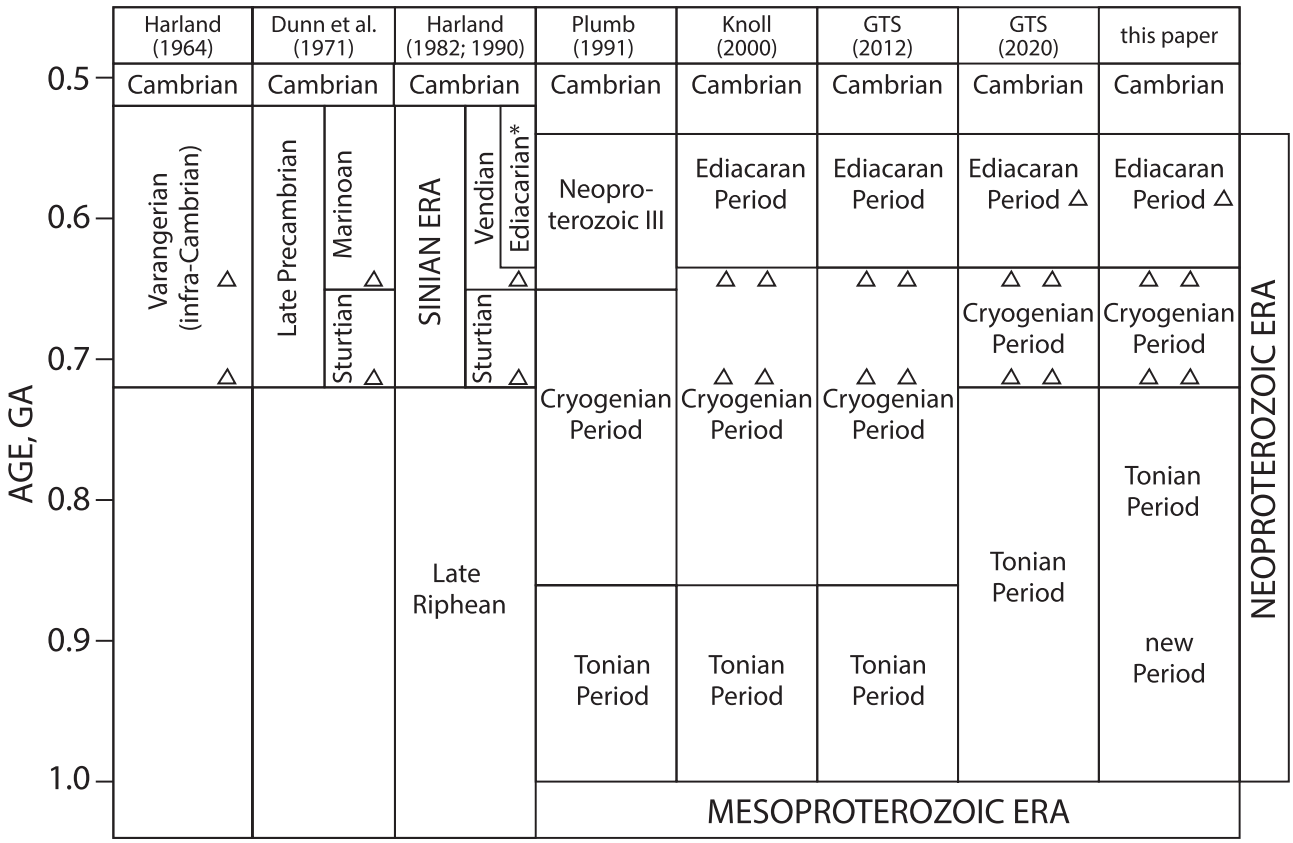

Fig. 5. Evolution of stratigraphic terminology for the Neoproterozoic Era. Note that age ranges for subdivisions on previous timescales are based on current age estimates. Triangle symbol (Δ) denotes the approximate levels of glaciations relevant to the timescale subdivisions. * denotes the term 'Ediacarian' introduced by Cloud and Glaessner (1982). Terminology after Dunn et al. (1971); Harland (1964, 1982, 1990); Plumb (1991); Van Kranendonk *et al.* (2012) (GTS 2012); Knoll (2000) Strachan *et al.* (2020) (GTS 2020) and this paper as indicated.

This term also originates from South Australia (the Ediacaran Hills) where Ediacara-type fossils were first recognized (Sprigg 1947). Plumb (1991) penned the name 'Cryogenian' for the period that included these widespread deposits and the term 'Tonian' (meaning stretching in Greek and in reference to the onset of rifting, now related to the break-up of Rodinia) for the preceding period, setting the chronological boundary between them at 850 Ma. These terms and GSSA boundaries were revised from previously suggested period-rank subdivisions on the geological timescale by the Subcommission on Precambrian Stratigraphy (Plumb and James 1986).

The number, duration, and intensity of the glaciations have been intensely debated (e.g. Kaufman *et al.* 1997; Kennedy *et al.* 1998; Halverson *et al.* 2005), particularly in the light of the Snowball Earth hypothesis (Hoffman *et al.* 1998; Hoffman and Schrag 2002; Etienne *et al.* 2007; Fairchild and Kennedy 2007). Notwithstanding these debates, the base of the Ediacaran System (Period) was formally ratified in 2004 in South Australia (Knoll *et al.* 2004, 2006*a*, *b*) at the same stratigraphic level as originally proposed by Cloud and Glaessner (1982) for their 'Ediacarian' period. The terms Cryogenian and Tonian are now widely accepted for the two preceding periods (Shields-Zhou *et al.* 2012, 2016), since a proliferation of radioisotopic ages has largely resolved the question of the number and timing of Neoproterozoic glaciations. It is now well established that two discrete glaciations of global extent occurred during the Cryogenian Period (i.e. between *c.* 717 and *c.* 635 Ma), separated by a non-glacial interval (Fig. 4). Despite initial reservations, the international community has generally adopted the terms *Sturtian* and *Marinoan* to refer to these two glacial episodes ('cryochrons', cf. Hoffman *et al.* 2017) of the Cryogenian Period. This subdivision, though still informal, appears justifiable in light of the geochronological evidence that (1) the Sturtian glaciation is now thought to have begun at *c.* 717 Ma (Macdonald *et al.* 2010, 2018; MacLennan *et al.* 2018) and ended at *c.* 660 Ma (Rooney *et al.* 2015, 2020; Cox *et al.* 2018; Wang *et al.* 2019) synchronously worldwide, within the uncertainty of available ages, and that (2) the Marinoan glaciation, though shorter-lived and of uncertain duration (between about 4 and 17 Ma; Hoffmann *et al.* 2004; Condon *et al.* 2005; Prave *et al.* 2016; Bao *et al.* 2018; Nelson *et al.* 2020) also ended synchronously at 635.5 Ma (Crockford *et al.* 2018; Zhou *et al.* 2019). The start of the Cryogenian Period has now been changed to *c.* 720 Ma (Shields-Zhou *et al.* 2016) so as to encompass only the glaciogenic sequences, pending proposal and ratification of a GSSP.

According to the current timescale (Fig. 1a), the preceding Tonian Period now lasts 280 million years. Having originally been envisaged to encapsulate a period of lithospheric thinning (supercontinent break-up), the Tonian covers the final amalgamation of Rodinia (Evans *et al.* 2016; Merdith *et al.* 2017*a*) and a prolonged interval of relative stability prior to the onset of major break-up after 0.83 Ga, and perhaps as late as 0.75 Ga (Jing *et al.* 2020; Merdith *et al.* 2017*b*). A proliferation of sedimentary basins in Rodinia between *c.* 850 and 800 Ma (e.g. the Centralian Superbasin of Australia, the East Svalbard–East Greenland basin, the Mackenzie Mountains–Amundsen and associated basins of northern-northwestern Canada, the Nanhua rift basin of South China and the Central Africa Copperbelt (Rainbird *et al.* 1996; Lindsay 2002; Bull *et al.* 2011; Wang *et al.* 2011; Hoffman *et al.* 2012; Li *et al.* 2013), were originally interpreted to record an initial phase of Rodinia break-up (Li *et al.* 1999; Macdonald *et al.* 2012), perhaps related to insulation of the underlying mantle (Lindsay 2002) and/or the influence of a series of similarly aged mantle

plumes and associated LIP events that impinged on Rodinia at this time (Li *et al.* 1999, 2004). The existence of widespread basin-scale evaporite deposits with ages ranging from *c.* 830 to 730 Ma (Lindsay 1987; Prince *et al.* 2019) is consistent with rifting around this time. Notwithstanding intracontinental rifting along the western margin of North America (e.g. Macdonald *et al.* 2012), evidence of extension leading to continental separation is lacking and true break-up probably began in earnest only around the start of the Cryogenian (e.g. Merdith *et al.* 2017*a*, *b*) or even in the Ediacaran Period (e.g. Tegner *et al.* 2019), followed by a peak in passive continental margin abundance at *c.* 600 Ma (Bradley 2008). Rodinia existence as a supercontinent therefore coincided with the currently defined Tonian Period, which was named for the tectonic stretching that led to its break-up.

Division of the long Tonian into two periods is therefore desirable, although at present most *c.* 850–800 Ma basins lack adequate geochronological control. The post-800 Ma Tonian fossil record is distinct from the pre-850 Ma record, and is marked by the first appearance of mineralized scales and vase-shaped microfossils in the fossil record, suggesting nascent stages of biomineralization and heterotrophic protistan evolution, but biostratigraphically useful fossils are currently too scarce to achieve any robust subdivision. We consider that a new period might conceivably cover the preceding interval of cratonization from the final amalgamation to initial rifting events, i.e. approximately ≤1.0 to ≥0.8 Ga, characterized by lower seawater Sr isotope values and relatively muted carbon isotopic values, followed by a revised Tonian Period from ≥0.8 to *c.* 0.72 Ga. We tentatively propose either of the terms *Kleisian* (Fig. 1c) or *Syndian*, following the Greek words respectively for the 'closure' or 'connection' that naturally followed the narrowing of oceans in the final assembly phase of Rodinia.

Concluding remarks and agreed recommendations

1) The history of the Earth and its geological record can reasonably be divided into its current four eons (Hadean, Archean, Proterozoic and Phanerozoic), whereby the Hadean–Archean boundary is taken to represent the start of the terrestrial rock record at *c.* 4.0 Ga.

2) Two first-order (*Archean and Proterozoic eon*) and six second-order (*Paleoarchean, Mesoarchean, Neoarchean, Paleoproterozoic, Mesoproterozoic, Neoproterozoic era*) stratigraphic intervals provide intuitive subdivision of post-Hadean to pre-Phanerozoic time. We consider that the Archean Eon would be more naturally subdivided into three informal units of equal duration (Fig. 1c) instead of the current four eras, to be defined further after detailed discussions by a commission of international experts.

3) Major transitions in Earth's tectonic, biological and environmental history occurred at approximately 2.5–2.3, 1.8–1.6 and 1.0–0.8 Ga. We consider, therefore, that current GSSAs at 2.5, 1.6 and 1.0 Ga could be replaced expeditiously by rock-based Proterozoic eras beginning at or after *c.* 2.45, 1.8 and 1.0 Ga, respectively, based around these major transitions, all of which occurred following orogenic peaks and during times of waning zircon production (post-acme, but not yet zenith) in line with Phanerozoic boundaries.

4) We suggest that current period-level GSSAs be replaced by improved rock-based concepts and interim chronostratigraphic units as soon as practicable, continuing recent progress towards that goal, illustrated, for example, by the establishment of an Ediacaran GSSP in 2004 and chronostratigraphic definition of the base of the Cryogenian at *c.* 720 Ma in 2016. Although all existing period names could be retained in a future chronostratigraphic scheme, some will need more conceptual underpinning, which would likely result in movement of the Siderian Period into the Archean Eon.

5) We recommend that a future Paleoproterozoic Era contain only three periods beginning at or after *c.* 2.45, 2.3 and 2.05 Ga, respectively, so that the era begins near the end of major Archean BIF deposition, the onset of widespread glaciation and the Great Oxidation Episode, but ends close to the onset of a prolonged period of cratonic, climatic and isotopic stability. We recommend that the Statherian Period be moved into the Mesoproterozoic Era. Future attention will likely focus on ensuring that rock-based periods (Siderian, Rhyacian and Orosirian) bracket the natural phenomena for which they were named (iron formation, magmatism and orogenies, respectively). Since we propose that the Siderian Period be moved into the Neoarchean, a new period, potentially the *Skourian* Period (Fig. 6b), would become the first period of the Paleoproterozoic Era.

6) We recommend that a revised Mesoproterozoic Era contain four periods (Statherian starting at *c.* 1.8 Ga, Calymmian at *c.* 1.6 Ga, Ectasian at *c.* 1.4 Ga and Stenian at *c.* 1.2 Ga) so that it begins after major orogenic climax, but before putative eukaryote-grade fossil assemblages, in the form of ornamented acritarchs and megascopic fronds, and ends after the Grenville Orogeny near the time of final stages of Rodinia supercontinent amalgamation.

7) We recommend that a revised Neoproterozoic Era contain four periods: a pre-Tonian period starting at *c.* 1.0 Ga, Tonian at *c.* 0.80 Ga, Cryogenian at *c.* 0.72 Ga and an Ediacaran Period, which has a ratified GSSP, dated at *c.* 635 Ma, so that it begins around the final amalgamation of Rodinia and ends traditionally at the Ediacaran–Cambrian boundary. We tentatively propose that the pre-Tonian period be named the *Kleisian* Period (Fig. 1c), although *Syndian* might also be considered.

8) These and further refinements of pre-Cryogenian time and strata could be developed by new expert subcommissions to cover the (1) pre-Ediacaran Neoproterozoic (currently, the Cryogenian Subcommission), (2) Mesoproterozoic, (3) Paleoproterozoic and (4) Archean and its boundary with the Hadean.

Acknowledgements The authors represent an international working group of the International Commission on Stratigraphy on pre-Cryogenian chronostratigraphic subdivision. We are greatly indebted to many people who have provided comments, encouragement and helpful advice on various drafts of this article from its early green paper stage, including the ICS executive officers David Harper, Brian Huber, Phil Gibbard and Shuzhong Shen, the IUGS general secretary Stan Finney, and the following people who commented on various draft versions Phil Donoghue, A.K. Jain, Vivek Kale, Mihir Deb, M. Jayananda, Jyotiranjan Ray, Aivo Lepland, Peter Haines, Thomas Vandyk and Martin Whitehouse. New period names were suggested by A. Bekker (*Scourian/Skourian*), D. Evans (*Kleisian, Syndian*) and G. Shields (*Kratian*). We thank Peter Cawood, Damian Nance for detailed review comments and Deta Gasser for helpful editorial advice that greatly improved the final manuscript.

Author contributions **GAS**: conceptualization (lead), writing – original draft (lead), writing – review & editing (lead); **RAS**: writing – original draft (equal), writing – review & editing (supporting); **SMP**: writing – original draft (equal), writing – review & editing (supporting); **GPH**: writing – original draft (equal), writing – review & editing (supporting); **FAM**: writing – review & editing (supporting); **KAP**: writing – review & editing (supporting); **CJA**: writing – review & editing (supporting); **DMB**: writing – review & editing (supporting); **AB**: writing – review & editing (supporting), writing – review & editing (supporting); **WB**: writing – review & editing (supporting); **AB**: writing – review & editing (supporting), writing – review & editing (supporting); **PPC**: writing – review & editing (supporting); **ASC**: writing – review & editing (supporting); **KC**: writing – review & editing (supporting); **KD**: writing – review & editing (supporting); **DAE**: writing – review & editing (supporting); **RE**: writing – review & editing (supporting); **AEF**: writing – review & editing (supporting); **HF**: writing – review & editing (supporting); **RF**: writing – review & editing (supporting); **PFH**: writing – review & editing (supporting); **BSK**: writing – review & editing (supporting); **ABK**: writing – review & editing (supporting); **RNM**: writing – review & editing (supporting); **DGP**: writing – review & editing (supporting); **SWP**: writing – review & editing (supporting); **RR**: writing – review & editing (supporting); **MS**: writing – review & editing (supporting); **CS**: writing – review & editing (supporting); **ES**: writing – review & editing (supporting); **RT**: writing – review & editing (supporting); **ET**: writing – review & editing (supporting); **SX**: writing – review & editing (supporting); **SZ**:

writing – review & editing (supporting); **YZ**: writing – review & editing (supporting); **MZ**: writing – review & editing (supporting)

Funding This research received no specific grant from any funding agency in the public, commercial, or not-for-profit sectors.

Data availability Data sharing is not applicable to this article as no datasets were generated or analysed during the current study.

Scientific editing by Deta Gasser

References

Adam, Z.R., Skidmore, M.L., Mogk, D.W. and Butterfield, N.J. 2017. A Laurentian record of the earliest fossil eukaryotes. *Geology*, **45**, 387–390, https://doi.org/10.1130/G38749.1

Alcott, L.J., Mills, B.J.W. and Poulton, S.W. 2019. Stepwise Earth oxygenation is an inherent property of global biogeochemical cycling. *Science*, **6471**, 1333–1337, https://doi.org/10.1126/science.aax6459

Allwood, A.C., Walter, M.R., Burch, I.W. and Kamber, B.S. 2007. 3.43 billion-year-old stromatolite reef from the Pilbara Craton of Western Australia: Ecosystem-scale insights to early life on Earth. *Precambrian Research*, **158**, 198–207, https://doi.org/10.1016/j.precamres.2007.04.013

Anbar, A.D., Duan, Y., *et al.* 2007. A whiff of oxygen before the Great Oxidation Event. *Science*, **317**, 1903–1906, https://doi.org/10.1126/science.1140325

Arndt, N.T. 2008. *Komatiite*. Cambridge University Press, Cambridge.

Arp, G., Reimer, A. and Reitner, J. 2001. Photosynthesis-induced biofilm calcification and calcium concentrations in Phanerozoic oceans. *Science*, **292**, 1701–1074, https://doi.org/10.1126/science.1057204

Ashwal, L.D. and Bybee, G.M. 2017. Crustal Evolution and the temporality of anorthosites. *Earth Science Reviews*, **173**, 307–330, https://doi.org/10.1016/j.earscirev.2017.09.002

Bao, X., Zhang, S., *et al.* 2018. Cyclostratigraphic constraints on the duration of the Datangpo Formation and the onset of the Nantuo (Marinoan) glaciation in South China. *Earth and Planetary Science Letters*, **483**, 52–63, https://doi.org/10.1016/j.epsl.2017.12.001

Bartley, J.K., Semikhatov, M.A., Kaufman, A.J., Knoll, A.H., Pope, M.C. and Jacobsen, S.B. 2001. Global events across the Mesoproterozoic–Neoproterozoic boundary: C and Sr isotopic evidence from Siberia. *Precambrian Research*, **111**, 165–202, https://doi.org/10.1016/S0301-9268(01)00160-7

Bédard, J.H. 2018. Stagnant lids and mantle overturns: Implications for Archean tectonics, magmagenesis, crustal growth, mantle evolution, and the start of plate tectonics. *Geoscience Frontiers*, **9**, 19–49, https://doi.org/10.1016/j.gsf.2017.01.005

Bekker, A. 2014. Great Oxygenation Event. *In*: Amils, R., *et al.* (eds) *Encyclopedia of Astrobiology*. Springer-Verlag, Berlin, 1–9.

Bekker, A. and Kaufman, A.J. 2007. Oxidative forcing of global climate change: a biogeochemical record across the oldest Paleoproterozoic ice age in North America. *Earth and Planetary Science Letters*, **258**, 486–499, https://doi.org/10.1016/j.epsl.2007.04.009

Bekker, A., Holland, H.D. *et al.* 2004. Dating the rise of atmospheric oxygen. *Nature*, **427**, 117–120, https://doi.org/10.1038/nature02260

Bekker, A., Slack, J.F., Planavsky, N., Krapez, B., Hofmann, A., Konhauser, K.O. and Rouxel, O.J. 2010. Iron formation: the sedimentary product of a complex interplay among mantle, tectonic, oceanic, and biospheric processes. *Economic Geology*, **105**, 467–508, https://doi.org/10.2113/gsecongeo.105.3.467

Bekker, A., Planavsky, N. *et al.* 2014. Iron formations: Their origins and implications for ancient seawater chemistry. *Treatise on Geochemistry*, **12**, 561–628, https://doi.org/10.1016/B978-0-08-095975-7.00719-1

Bekker, A., Krapež, B. and Karhu, J.A. 2020. Correlation of the stratigraphic cover of the Pilbara and Kaapvaal cratons recording the lead up to Paleoproterozoic Icehouse and the GOE. *Earth Science Reviews*, **211**, 103389, https://doi.org/10.1016/j.earscirev.2020.103389

Bekker, A., Krapež, B., Karhu, J.A. and Chamberlain, K. 2021. Reply to comment on 'Bekker, A., Krapež, B., Karhu, J.A., 2020. Correlation of the stratigraphic cover of the Pilbara and Kaapvaal cratons recording the lead up to Paleoproterozoic Icehouse and the GOE. Earth-Science Reviews, 211, 103389' by Pascal Philippot, Bryan A. Killingsworth, Jean-Louis Paquette, Svetlana Tessalina, Pierre Cartigny, Stefan V. Lalonde, Christophe Thomazo, Janaina N. Ávila, Vincent Busigny. *Earth-Science Reviews*, https://doi.org/10.1016/j.earscirev.2021.103607

Bengtson, S., Sallstedt, T., Belivanova, V. and Whitehouse, M. 2017. Three-dimensional preservation of cellular and subcellular structures suggests 1.6 billion-year-old crown-group red algae. *PLoS Biology*, **15**, e2000735, https://doi.org/10.1371/journal.pbio.2000735

Berney, C. and Pawlowski, J. 2006. A molecular time-scale for eukaryote evolution recalibrated with the continuous microfossil record. *Proceedings of the Royal Society B*, **273**, 1867–1872, https://doi.org/10.1098/rspb.2006.3537

Betts, H.C., Puttick, M.N., Clark, J.W., Williams, T.A., Donoghue, P.C.J. and Pisani, D. 2018. Integrated genomic and fossil evidence illuminates life's early evolution and eukaryote origin. *Nature Ecology & Evolution*, **2**, 1556–1562, https://doi.org/10.1038/s41559-018-0644-x

Bingen, B., Viola, G., Möller, C., Auwera, J.V., Laurent, A. and Yi, K. 2021. The Sveconorwegian Orogeny. *Gondwana Research*, **90**, 273–313, https://doi.org/10.1016/j.gr.2020.10.014

Blank, C.E. 2013. Origin and early evolution of photosynthetic eukaryotes in freshwater environments: reinterpreting Proterozoic paleobiology and biogeochemical processes in light of trait evolution. *Journal of Phycology*, **49**, 1040–1055, https://doi.org/10.1111/jpy.12111

Blättler, C.L., Claire, M.W., Prave, A.R., Kirsimäe, K., Higgins, J.A. and Medvedev, P.V. 2018. Two-billion-year-old evaporites capture Earth's great oxidation. *Science*, **360**, 320–323, https://doi.org/10.1126/science.aar2687

Bleeker, W. 2003. The late Archean record: a puzzle in c. 35 pieces. *Lithos*, **71**, 99–134, https://doi.org/10.1016/j.lithos.2003.07.003

Bleeker, W. 2004*a*. Towards a 'natural' Precambrian time scale. *In*: Gradstein, F.M., Ogg, J.G. and Smith, A.G. (eds) *A Geologic Time Scale 2004*. Cambridge University Press, Cambridge, 141–146.

Bleeker, W. 2004*b*. Towards a 'natural' time scale for the Precambrian – A proposal. *Lethaia*, 219–222, https://doi.org/10.1080/00241160410006456

Bleeker, W., Ketchum, J.W.F., Jackson, V.A. and Villeneuve, M.E. 1999. The Central Slave Basement Complex, Part 1: Its structural topology and autochthonous cover. *Canadian Journal of Earth Sciences*, **36**, 1083–1109, https://doi.org/10.1139/e98-102

Bodorkos, S., Crowley, J.L., Claoue-Long, J.C., Anderson, J.R. and Magee, C.W. Jr. 2021. Precise U–Pb baddelyite dating of the Derim Derim dolerite, McArthur Basin, Northern Territory: old and new SHRIMP and ID-TIMS constraints. *Australian Journal of Earth Sciences*, **68**, 36–50, https://doi.org/10.1080/08120099.2020.1749929

Bowring, S.A. and Grotzinger, J.P. 1992. Implications of new chronostratigraphy for tectonic evolution of Wopmay orogen, northwest Canadian Shield. *American Journal of Science*, **292**, 1–20, https://doi.org/10.2475/ajs.292.1.1

Bowring, S.A. and Williams, I.S. 1999. Priscoan (4.00–4.03 Ga) orthogneisses from northwestern, Canada. *Contributions Mineralogy and Petrology*, **134**, 3–16, https://doi.org/10.1007/s004100050465

Bradley, D.C. 2008. Passive margins through earth history. *Earth-Science Reviews*, **91**, 1–26, https://doi.org/10.1016/j.earscirev.2008.08.001

Brasier, M.D. and Lindsay, J.F. 1998. A billion years of environmental stability and the emergence of the eukaryotes: new data from northern Australia. *Geology*, **26**, 555–558, https://doi.org/10.1130/0091-7613(1998)026<0555:ABYOES>2.3.CO;2

Brasier, M., Cowie, J. and Taylor, M. 1994. Decision on the Precambrian–Cambrian boundary stratotype. *Episodes*, **17**, 3–8, https://doi.org/10.18814/epiiugs/1994/v17i1.2/002

Brasier, A.T., Fallick, A.E., Prave, A.R., Melezhik, V.A., Lepland, A. and FAR-DEEP scientists 2011. Coastal sabkha dolomites and calcitised sulphates preserving the Lomagundi-Jatuli carbon isotope signal. *Precambrian Research*, **189**, 193–211, https://doi.org/10.1016/j.precamres.2011.05.011

Brasier, A.T., Martin, A.P., Melezhik, V.A., Prave, A.R., Condon, D.J. and Fallick, A.E. 2013. Earth's earliest global glaciation? Carbonate geochemistry and geochronology of the Polisarka Sedimentary Formation, Kola Peninsula, Russia. *Precambrian Research*, **235**, 278–294, https://doi.org/10.1016/j.precamres.2013.06.007

Brocks, J.J. 2018. The transition from a cyanobacterial to algal world and the emergence of animals. *Emerging Topics in Life Sciences*, **2**, 181–190, https://doi.org/10.1042/ETLS20180039

Buick, R., Des Marais, D.J. and Knoll, A.H. 1995. Stable isotope compositions of carbonates from the Mesoproterozoic Bangemall Group, northwestern Australia. *Chemical Geology*, **123**, 153–171, https://doi.org/10.1016/0009-2541(95)00049-R

Bull, S., Selley, D., Broughton, D., Hitzman, M., Cailteux, J., Large, R. and McGoldrick, P. 2011. Sequence and carbon isotopic stratigraphy of the Neoproterozoic Roan Group strata of the Zambian copperbelt. *Precambrian Research*, **190**, 70–89, https://doi.org/10.1016/j.precamres.2011.07.021

Butterfield, N.J. 2000. *Bangiomorphapubescens* n. gen., n. sp.: implications for the evolution of sex, multicellularity, and the Mesoproterozoic radiation of eukaryotes. *Paleobiology*, **26**, 386–404, https://doi.org/10.1666/0094-8373(2000)026<0386:BPNGNS>2.0.CO;2

Butterfield, N.J. 2004. A vaucheriacean alga from the middle Neoproterozoic of Spitsbergen: implications for the evolution of Proterozoic eukaryotes and the Cambrian explosion. *Paleobiology*, **30**, 231–252, https://doi.org/10.1666/0094-8373(2004)030<0231:AVAFTM>2.0.CO;2

Butterfield, N.J., 2015. The Neoproterozoic. *Current Biology*, **25**, R859–863.

Butterfield, N.J., Knoll, A.H. and Swett, K. 1994. Paleobiology of the Neoproterozoic Svanbergfjellet Formation, Spitsbergen. *Fossils and Strata*, **34**, 1–84.

Canfield, D.E. 1998. A new model for Proterozoic ocean chemistry. *Nature*, **396**, 450–453, https://doi.org/10.1038/24839

Canfield, D.E., Zhang, S. *et al.* 2018. A Mesoproterozoic iron formation. *PNAS*, **115**, E3895–E3904, https://doi.org/10.1073/pnas.1720529115

Cawood, P.A. and Hawkesworth, C.J. 2014. Earth's middle age. *Geology*, **42**, 503–506, https://doi.org/10.1130/G35402.1

Cawood, P.A. and Pisarevsky, S.A. 2017. Laurentia–Baltica–Amazonia relations during Rodinia assembly. *Precambrian Research*, **292**, 386–397, https://doi.org/10.1016/j.precamres.2017.01.031

Cawood, P.A., Hawkesworth, C.J. and Dhuime, B. 2013. The continental record and the generation of continental crust. *Geological Society of America Bulletin*, **125**, 14–32, https://doi.org/10.1130/B30722.1

Cawood, P.A., Hawkesworth, C.J., Pisarevsky, S.A., Dhuime, B., Capitanio, F.A. and Nebel, O. 2018. Geological archive of the Onset of Plate Tectonics. *Philosophical Transactions of the Royal Society A*, **376**, 20170405, https://doi.org/10.1098/rsta.2017.0405

Chakraborty, P.P., Mukhopadhyay, J., Paul, P., Banerjee, D.M. and Bera, M.K. 2020. Early atmosphere and hydrosphere oxygenation: Clues from Precambrian paleosols and chemical sedimentary records of India. *Episodes*, **43**, 175–186, https://doi.org/10.18814/epiiugs/2020/020011

Chemale, F., Dussin, I.A., Alkmim, F.F., Martins, M.S., Queiroga, G., Armstrong, R. and Santos, M.N. 2012. Unravelling a Proterozoic basin history through detrital zircon geochronology: The case of the Espinhaço Supergroup, Minas Gerais, Brazil. *Gondwana Research*, **22**, 200–206, https://doi.org/10.1016/j.gr.2011.08.016

Cloud, P. 1972. A working model of the primitive Earth. *American Journal of Science*, **272**, 537–548, https://doi.org/10.2475/ajs.272.6.537

Cloud, P. 1976. Major features of crustal evolution. *Geological Society of South Africa, Alexander L. du Toit Memorial Lecture Series*, **14**, 33.

Cloud, P. and Glaessner, M.F. 1982. The Ediacarian Period and System: Metazoa inherit the Earth. *Science*, **217**, 783–792, https://doi.org/10.1126/science.217.4562.783

Cohen, P.A. and Knoll, A.H. 2012. Scale Microfossils from the Mid-Neoproterozoic Fifteenmile Group, Yukon Territory. *Journal of Paleontology*, **86**, 775–800, https://doi.org/10.1666/11-138.1

Cohen, P.A. and Macdonald, F.A. 2015. The Proterozoic record of eukaryotes. *Paleobiology*, **41**, 610–632, https://doi.org/10.1017/pab.2015.25

Cohen, P.A., Irvine, S.W. and Strauss, J.V. 2017*a*. Vase-shaped microfossils from the TonianCallison Lake Formation of Yukon, Canada: taxonomy, taphonomy and stratigraphic palaeobiology. *Palaeontology*, **60**, 683–701, https://doi.org/10.1111/pala.12315

Cohen, P.A., Strauss, J.V., Rooney, A.D., Sharma, M. and Tosca, N. 2017*b*. Controlled hydroxyapatite biomineralization in an 810 million-year-old unicellular eukaryote. *Science Advances*, **3**, e1700095, https://doi.org/10.1126/sciadv.1700095

Collins, A.S., Patranabis-Deb, S., *et al.* 2015. Detrital mineral age, radiogenic isotopic stratigraphy and tectonic significance of the Cuddapah Basin, India. *Gondwana Research*, **28**, 1294–1309, https://doi.org/10.1016/j.gr.2014.10.013

Condie, K.C. 1998. Episodic continental growth and supercontinents: a mantle avalanche connection? *Earth and Planetary Science Letters*, **163**, 97–108, https://doi.org/10.1016/S0012-821X(98)00178-2

Condie, K.C. 2004. Supercontinents and superplume events: distinguishing signals in the geologic record. *Physics of the Earth and Planetary Interiors*, **146**, 319–332, https://doi.org/10.1016/j.pepi.2003.04.002

Condie, K.C. 2014. Growth of continental crust: a balance between preservation and recycling. *Mineralogical Magazine*, **78**, 623–637, https://doi.org/10.1180/minmag.2014.078.3.11

Condie, K.C. and Aster, R.C. 2010. Episodic zircon age spectra of orogenic granitoids: the supercontinent connection and continental growth. *Precambrian Research*, **180**, 227–236, https://doi.org/10.1016/j.precamres.2010.03.008

Condie, K.C. and Puetz, S.J. 2019. Time series analysis of mantle cycles II: The geologic record in zircons, large igneous provinces and mantle lithosphere. *Geoscience Frontiers*, **10**, 1327–1336, https://doi.org/10.1016/j.gsf.2019.03.005

Condie, K.C., O'Neill, C. and Aster, R.C. 2009. Evidence and implications for a widespread magmatic shutdown for 250 Ma on Earth. *Earth and Planetary Science Letters*, **282**, 294–298, https://doi.org/10.1016/j.epsl.2009.03.033

Condon, D., Zhu, M., Bowring, S., Jin, Y., Wang, W. and Yang, A. 2005. From the Marinoan glaciation to the oldest bilaterians: U–Pb ages from the Doushantuo Formation, China. *Science*, **308**, 95–98, https://doi.org/10.1126/science.1107765

Cornell, D.H., Thomas, R.J., Gibson, R., Moen, H.F.G., Moore, J.M. and Reid, D.L. 2006. Namaqua-Natal Province. *In*: Johnson, M.R., Anhauesser, C.R. and Thomas, R.J. (eds) *The Geology of South Africa.* Johannesburg/Council for Geoscience, Pretoria, 325–379.

Cornet, Y., François, C., Compère, P., Callec, Y., Roberty, S., Plumier, J.C. and Javaux, E.J. 2019. New insights on the paleobiology, biostratigraphy and paleogeography of the pre-Sturtian microfossil index taxon *Cerebrosphaera*. *Precambrian Research*, **332**, 105410, https://doi.org/10.1016/j.precamres.2019.105410

Cox, G.M., Halverson, G.P. *et al.* 2016. Continental flood basalt weathering as a trigger for Neoproterozoic Snowball Earth. *Earth and Planetary Science Letters*, **446**, 89–99, https://doi.org/10.1016/j.epsl.2016.04.016

Cox, G.M., Isakson, V. *et al.* 2018. South Australian U–Pb zircon (CA-ID-TIMS) age supports globally synchronous Sturtian deglaciation. *Precambrian Research*, **315**, 257–263, https://doi.org/10.1016/j.precamres.2018.07.007

Cramer, B.D. and Jarvis, I. 2020. Carbon isotope stratigraphy. *In*: Gradstein, F.M., Ogg, J.G., Schmitz, M.D. and Ogg, G.M. (eds) *The Geologic Time Scale 2020*. Elsevier Science, **1**, 309–343.

Crockford, P.W., Hodgskiss, M.S.W., Uhlein, G.J., Caxito, F., Hayles, J.A. and Halverson, G.P. 2018. Linking paleocontinents through is $\Delta^{17}O$ anomalies. *Geology*, **46**, 179–182, https://doi.org/10.1130/G39470.1

Crockford, P.W., Kunzmann, M., *et al.* 2019. Claypool continued: extending the isotopic record of sedimentary sulfate. *Chemical Geology*, **514**, 200–225, https://doi.org/10.1016/j.chemgeo.2019.02.030

Crosby, C.H., Bailey, J.V. and Sharma, M. 2014. Fossil evidence of iron-oxidizing chemolithotrophy linked to phosphogenesis in the wake of the Great Oxidation Event. *Geology*, **42**, 1015–1018, https://doi.org/10.1130/G35922.1

Crook, K.A.W. 1989. Why the Precambrian time-scale should be chronostratigraphic: A response to recommendations by the Subcommission on Precambrian stratigraphy. *Precambrian Research*, **43**, 143–150, https://doi.org/10.1016/0301-9268(89)90009-0

Dana, J.D. 1872. *American Journal of Science and Arts*, 3rd series, **3**, 250–257, https://doi.org/10.2475/ajs.s3-3.16.250

Donnadieu, Y., Goddéris, Y., Ramstein, G. and Nédélec, A. 2004. A 'snowball Earth' climate triggered by continental break-up through changes in runoff. *Nature*, **428**, 303–306, https://doi.org/10.1038/nature02408

Dunn, P.R., Plumb, K.A. and Roberts, H.G. 1966. A proposal for time-stratigraphic classification of the Australian Precambrian. *Journal of the Geological Society of Australia*, **13**, 593–608, https://doi.org/10.1080/00167616608728634

Dunn, P., Thomson, B. and Rankama, K. 1971. Late Pre-Cambrian glaciation in Australia as a stratigraphic boundary. *Nature*, **231**, 498–502, https://doi.org/10.1038/231498a0

Eme, L., Sharpe, S.C., Brown, M.W. and Roger, A.J. 2014. On the age of eukaryotes: evaluating evidence from fossils and molecular clocks. *Cold Spring Harbor Perspectives in Biology*, **6**, a016139, https://doi.org/10.1101/cshperspect.a016139

Ernst, R.E. and Youbi, N. 2017. How large igneous provinces affect global climate, sometimes cause mass extinctions, and represent natural markers in the geological record. *Palaeogeography, Palaeoclimatology, Palaeoecology*, **478**, 30–52, https://doi.org/10.1016/j.palaeo.2017.03.014

Ernst, R.E., Bond, D.P.G. and Zhang, S.H. 2020. Influence of Large Igneous Provinces. *In*: Gradstein, F.M., Ogg, J.G., Schmitz, M.D. and Ogg, G.M. (eds) *The Geologic Time Scale 2020*. Elsevier Science, **2**, 345–356.

Etienne, J.L., Allen, P.A., Rieu, R. and Le Guerroué, E. 2007. Neoproterozoic glaciated basins: a critical review of the Snowball Earth hypothesis by comparison with Phanerozoic basins. *In*: Hambrey, M.J., Christoffersen, P., Glasser, N.F. and Hubbard, B. (eds) *Glacial Sedimentary Processes and Products*. International Association of Sedimentologists Special Publication, **39**, 343–399.

Evans, D.A.D. and Mitchell, R.N. 2011. Assembly and breakup of the core of Paleoproterozoic–Mesoproterozoic supercontinent Nuna. *Geology*, **39**, 443–446, https://doi.org/10.1130/G31654.1

Evans, D.A.D., Beukes, N.J. and Kirschvink, J.L. 1997. A Paleoproterozoic Snowball Earth. *Nature*, **386**, 262–266, https://doi.org/10.1038/386262a0

Evans, D.A.D., Trindade, R.I.F., *et al.* 2016. Return to Rodinia? Moderate to high palaeolatitude of the São Francisco/Congo craton at 920 Ma. *Geological Society, London, Special Publications*, **424**, 167–190, https://doi.org/10.1144/SP424.1

Evans, D.A.D., Smirnov, A.N. and Gumsley, A.P. 2017. Paleomagnetism and U–Pb geochronology of the Black Range dykes, Pilbara Craton, Western Australia: a Neoarchean crossing of the polar circle. *Australian Journal of Earth Sciences*, **64**, 225–237, https://doi.org/10.1080/08120099.2017.1289981

Fairchild, I.J. and Kennedy, M.J. 2007. Neoproterozoic glaciation in the Earth system. *Journal of the Geological Society, London*, **164**, 895–921, https://doi.org/10.1144/0016-76492006-191

Fareeduddin and Banerjee, D.M. 2020. Aravalli craton and its mobile belts: An update. *Episodes*, **43**, 88–108, https://doi.org/10.18814/epiiugs/2020/020005

Farquhar, J., Bao, H. and Thiemens, M. 2000. Atmospheric influence of Earth's earliest sulphur cycle. *Science*, **289**, 756–758, https://doi.org/10.1126/science.289.5480.756

Fernandez-Alonso, M., Cutten, H., De Waele, B., Tack, L., Taho, A., Baudet, D. and Barritt, S.D. 2012. The Mesoproterozoic Karagwe-Ankole Belt (formerly the NE Kibara Belt): The result of prolonged extensional intracratonic basin development punctuated by two short-lived far-field compressional events. *Precambrian Research*, **216–219**, 63–86, https://doi.org/10.1016/j.precamres.2012.06.007

Fitzsimons, I.C.W. 2000. Grenville-age basement provinces in East Antarctica: evidence for three separate collisional orogens. *Geology*, **28**, 879–882, https://doi.org/10.1130/0091-7613(2000)28<879:GBPIEA>2.0.CO;2

Fralick, P. and Riding, R. 2015. Steep Rock Lake: Sedimentology and geochemistry of an Archean carbonate platform. *Earth-Science Reviews*, **151**, 132–175, https://doi.org/10.1016/j.earscirev.2015.10.006

Fralick, P., Davis, D.W. and Kissin, S.A. 2002. The age of the Gunflint Formation, Ontario, Canada: single zircon U–Pb age determinations from reworked volcanic ash. *Canadian Journal of Earth Sciences*, **39**, 1085–1091, https://doi.org/10.1139/e02-028

Frimmel, H.E. 2005. Archaean atmospheric evolution: evidence from the Witwatersrand gold fields, South Africa. *Earth Science Reviews*, **70**, 1–46, https://doi.org/10.1016/j.earscirev.2004.10.003

Frimmel, H.E. 2019. The Witwatersrand Basin and its gold deposits. *In*: Kröner, A. and Hofmann, A. (eds) *The Archaean Geology of the Kaapvaal Craton, Southern Africa*. Springer Nature, Cham, 255–275.

George, B.G., Ray, J.S., Shukla, A.D., Chatterjee, A., Awasthi, N. and Laskar, A.H. 2018. Stratigraphy and geochemistry of the Balwan Limestone, Vindhyan Supergroup, India: Evidence for the Bitter Springs $\delta^{13}C$ anomaly. *Precambrian Research*, **313**, 18–30, https://doi.org/10.1016/j.precamres.2018.05.008

Gibson, T.M., Wörndle, S., Crockford, P.W., Bui, T.H., Creaser, R.A. and Halverson, G.P. 2019. Radiogenic isotope chemostratigraphy reveals marine and nonmarine depositional environments in the late Mesoproterozoic Borden Basin, Arctic Canada. *Geological Society of America Bulletin*, **131**, 1965–1978, https://doi.org/10.1130/B35060.1

Gibson, G.M., Champion, D.C., Huston, D.L. and Withnall, I.W. 2020. Orogenesis in Paleo-Mesoproterozoic Eastern Australia: A response to arc–continent and continent–continent collision during assembly of the Nuna supercontinent. *Tectonics*, **39**, e2019TC005717, https://doi.org/10.1029/2019TC005717

Glaessner, M.F. 1962. Pre-Cambrian fossils. *Biological Reviews*, **37**, 467–494, https://doi.org/10.1111/j.1469-185X.1962.tb01331.x

Goldich, S.S. 1968. Geochronology in the Lake Superior region. *Canadian Journal of Earth Science*, **5**, 715–724, https://doi.org/10.1139/e68-070

Grenholm, M. and Schersten, A. 2015. A hypothesis for Proterozoic–Phanerozoic supercontinent cyclicity, with implications for mantle convection, plate tectonics and Earth system evolution. *Tectonophysics*, **662**, 434–453, https://doi.org/10.1016/j.tecto.2015.04.009

Grey, K., Hill, A.C. and Calver, C. 2011. Biostratigraphy and stratigraphic subdivision of Cryogenian successions of Australia in a global context. *Geological Society, London, Memoirs*, **36**, 113–134, https://doi.org/10.1144/M36.8

Griffin, W.L., Belousova, E.A., *et al.* 2014. The world turns over: Hadean–Archean crust-mantle evolution. *Lithos*, **189**, 2–15, https://doi.org/10.1016/j.lithos.2013.08.018

Grotzinger, J.P. 1990. Geochemical model for Proterozoic stromatolite decline. *American Journal of Science*, **290-A**, 80–103.

Guadagnin, F., Chemale Jr., F., Magalhães, J., Santana, A., Dussin, I. and Takehara, L. 2015. Age constraints on crystal-tuff from the Espinhaço Supergroup – insight into the Paleoproterozoic to Mesoproterozoic intracratonic basin cycles of the Congo-São Francisco Craton. *Gondwana Research*, **27**, 363–376, https://doi.org/10.1016/j.gr.2013.10.009

Gumsley, A.P., Chamberlain, K.R., Bleeker, W., Söderlund, U., de Kock, M.O., Larsson, E.R. and Bekker, A. 2017. Timing and tempo of the Great Oxidation Event. *PNAS*, **114**, 1811–1816, https://doi.org/10.1073/pnas.1608824114

Gumsley, A., Stamsnijder, J., *et al.* 2020. Neoarchean large igneous provinces on the Kaapvaal Craton in southern Africa re-define the formation of the Ventersdorp Supergroup and its temporal equivalents. *Geological Society of America Bulletin*, **132**, 1829–1844, https://doi.org/10.1130/B35237.1

Halverson, G.P. 2006. A Neoproterozoic chronology. *In*: Xiao, S. and Kaufman, A. (eds) *Neoproterozoic Geobiology and Paleobiology. Topics in Geobiology*, *27*. Springer, Dordrecht, the Netherlands, 231–271.

Halverson, G.P., Hoffman, P.F., Schrag, D.P., Maloof, A.C. and Rice, A.H. 2005. Towards a Neoproterozoic composite carbon isotope record. *Geological Society of America Bulletin*, **117**, 1181–1207, https://doi.org/10.1130/B25630.1

Halverson, G.P., Kunzmann, M., Strauss, J.V. and Maloof, A.C. 2018. The Tonian–Cryogenian transition in Svalbard. *Precambrian Research*, **319**, 79–95, https://doi.org/10.1016/j.precamres.2017.12.010

Halverson, G.P., Porter, S.M. and Shields, G.A. 2020. The Tonian and Cryogenian periods. *In*: Gradstein, F.M., Ogg, J.G., Schmitz, M.D. and Ogg, G.M. (eds) *The Geologic Time Scale 2020*. Elsevier Science, **1**, 495–519.

Han, T. and Runnegar, B. 1992. Megascopic eukaryotic algae from the 2.1-billion-year-old Negaunee Iron-Formation, Michigan. *Science*, **257**, 232–235, https://doi.org/10.1126/science.1631544

Hardisty, D.S., Lu, Z., *et al.* 2017. Perspectives on Proterozoic surface ocean redox from iodine contents in ancient and recent carbonate. *Earth and Planetary Science Letters*, **463**, 159–170, https://doi.org/10.1016/j.epsl.2017.01.032

Harland, W. 1964. Critical evidence for a great infra-Cambrian glaciation. *Geologische Rundschau*, **54**, 45–61, https://doi.org/10.1007/BF01821169

Harland, W.B., Cox, A.V., Llewellyn, P.G., Pickton, C.A.G., Smith, A.G. and Walters, R. 1982. *A Geologic Time Scale*. Cambridge University Press.

Harland, W.B., Armstrong, R.L., Cox, A.V., Craig, L.E., Smith, A.G. and Smith, D.G. 1990. *A Geologic Time Scale 1989*. Cambridge University Press.

Harper, D.A.T., Huber, B.T. and Gibbard, P.L. 2019. *International Union of Geological Sciences 2019 Annual Report*. IUGS General Secretariat, Beijing, 36–38.

Hawkesworth, C.J., Cawood, P.A. and Dhuime, B. 2016. Tectonics and crustal evolution. *GSA Today*, **26**, 4–11, https://doi.org/10.1130/GSATG272A.1

Hazen, R.M. 2010. The evolution of minerals. *Scientific American*, **303**, 58–65, https://doi.org/10.1038/scientificamerican0310-58

Hazen, R.M., Bekker, A., *et al.* 2011. Needs and opportunitires in mineral evolution research. *American Mineralogist*, **96**, 953–963, https://doi.org/10.2138/am.2011.3725

Hedberg, H. 1974. Basis for chronostratigraphic classification of the Precambrian. *Precambrian Research*, **1**, 165–177, https://doi.org/10.1016/0301-9268(74)90008-4

Heubeck, C. and Lowe, D.R. 1994. Depositional and tectonic setting of the Archean Moodies Group, Barberton greenstone belt, South Africa. *Precambrian Research*, **68**, 257–290, https://doi.org/10.1016/0301-9268(94)90033-7

Hickman, A.H. 2004. Two contrasting granite-greenstone terranes in the Pilbara craton, Australia: Evidence for vertical *and* horizontal tectonic regimes prior to 2900 Ma. *Precambrian Research*, **131**, 153–172, https://doi.org/10.1016/j.precamres.2003.12.009

Hill, A.C. and Walter, M.R. 2000. Mid-Neoproterozoic (*c.* 830–750 Ma) isotope stratigraphy of Australia and global correlation. *Precambrian Research*, **100**, 181–211, https://doi.org/10.1016/S0301-9268(99)00074-1

Hodgskiss, M.S.W., Crockford, P.W., Peng, Y., Wing, B.A. and Horner, T.J. 2019. A productivity collapse to end Earth's Great Oxidation. *PNAS*, **116**, 17207–17212, https://doi.org/10.1073/pnas.1900325116

Hodgskiss, M.S.W., Kunzmann, M., Poirier, A. and Halverson, G.P. 2018. The role of microbial iron reduction in the formation of Proterozoic molar tooth structures. *Earth and Planetary Science Letters*, **482**, 1–11, https://doi.org/10.1016/j.epsl.2017.10.037

Hofmann, H.J. 1975. Precambrian microflora, Belcher Islands, Canada: significance and systematics. *Journal of Paleontology*, **50**, 1040–1071.

Hofmann, H.J. 1990. Precambrian time units and nomenclature – the geon concept. *Geology*, **18**, 340–341, https://doi.org/10.1130/0091-7613(1990)018<0340:PTUANT>2.3.CO;2

Hofmann, H.J. 1992. New Precambrian time scale: Comments. *Episodes*, **15**, 122–123.

Hoffman, P.F. 1989. Speculations on Laurentia's first gigayear (2.0 to 1.0 Ga). *Geology*, **17**, 135–138, https://doi.org/10.1130/0091-7613(1989)017<0135:SOLSFG>2.3.CO;2

Hoffman, P.F. 1997. Tectonic genealogy of North America. *In*: van der Pluijm, B.A. and Marshak, S. (eds) *Earth Structure: An Introduction to Structural Geology and Tectonics*. McGraw-Hill, New York, 459–464.

Hoffman, P.F. 2014. The origin of Laurentia: Rae craton as the backstop for proto-Laurentian amalgamation by slab suction. *Geoscience Canada*, **41**, 313–320, https://doi.org/10.12789/geocanj.2014.41.049

Hoffman, P.F. and Schrag, D.P. 2002. The snowball Earth hypothesis: testing the limits of global change. *Terra Nova*, **14**, 129–155, https://doi.org/10.1046/j.1365-3121.2002.00408.x

Hoffman, P., Kaufman, A. and Halverson, G. 1998. Comings and goings of global glaciations on a Neoproterozoic tropical platform in Namibia. *GSA Today*, **8**, 1–9.

Hoffman, P.F., Halverson, G.P., Domack, E.W., Maloof, A.C., Swanson-Hysell, N.L. and Cox, G.M. 2012. Cryogenian glaciations on the southern tropical paleomargin of Laurentia (NE Svalbard and East Greenland), and a primary origin for the upper Russøya (Islay) carbon isotope excursion. *Precambrian Research*, **206–207**, 137–158, https://doi.org/10.1016/j.precamres.2012.02.018

Hoffman, P.F., Abbott, D.S., *et al.* 2017. Snowball Earth climate dynamics and Cryogenian geology and geobiology. *Science Advances*, **3**, e1600983, https://doi.org/10.1126/sciadv.1600983

Hoffmann, K.H., Condon, D.J., Bowring, S.A. and Crowley, J.L. 2004. A U–Pb zircon date from the Neoproterozoic Ghaub Formation, Namibia: Constraints on Marinoan glaciation. *Geology*, **32**, 817–820, https://doi.org/10.1130/G20519.1

Holland, H.D. 1984. *The Chemical Evolution of the Atmosphere and Oceans*. Princeton University Press, Princeton.

Holland, H.D. 2006. The oxygenation of the atmosphere and oceans. *Philosophical Transactions of the Royal Society B*, **361**, 903–915, https://doi.org/10.1098/rstb.2006.1838

Horton, F. 2015. Did phosphorus derived from the weathering of large igneous provinces fertilize the Neoproterozoic ocean? *Geochemistry, Geophysics, Geosystems*, **16**, 1723–1738, https://doi.org/10.1002/2015GC005792

Howchin, W. 1901. Preliminary note on the evidence of glacial beds of Cambrian age in South Australia. *Transactions of the Royal Society of South Australia*, **25**, 10–13.

James, H.L. 1972. Note 40 – Subdivision of Precambrian: an interim scheme to be used by U.S. Geological Survey. *AAPG Bulletin*, **56**, 1128–1133.

James, H.L. 1978. Subdivision of the Precambrian – a brief review and a report on recent decisions by the Subcommissionon Precambrian Stratigraphy. *Precambrian Research*, **7**, 193–204, https://doi.org/10.1016/0301-9268(78)90038-4

James, N.P., Narbonne, G.M. and Sherman, A.G. 1998. Molar-tooth carbonates: shallow subtidal facies of the mid- to late Proterozoic. *Journal of Sedimentary Research*, **68**, 716–722, https://doi.org/10.2110/jsr.68.716

Javaux, E.J. and Knoll, A.H. 2017. Micropaleontology of the lower Mesoproterozoic Roper Group, Australia, and implications for early eukaryotic evolution. *Journal of Paleontology*, **91**, 199–229, https://doi.org/10.1017/jpa.2016.124

Javaux, E.J. and Lepot, K. 2018. The Paleoproterozoic fossil record: Implications for the evolution of the biosphere during Earth's middle-age. *Earth Science Reviews*, **176**, 68–86, https://doi.org/10.1016/j.earscirev.2017.10.001

Javaux, E.J., Knoll, A.H. and Walter, M.R. 2001. Morphological and ecological complexity in early eukaryotic ecosystems. *Nature*, **412**, 66–69, https://doi.org/10.1038/35083562

Javaux, E.J., Marshall, C.P. and Bekker, A. 2010. Organic-walled microfossils in 3.2-billion-year-old shallow-marine siliciclastic deposits. *Nature*, **463**, 934–938, https://doi.org/10.1038/nature08793

Jing, X., Yang, Z., Evans, D.A.D., Tong, Y., Xi, Y. and Wang, H. 2020. A pan-latitudinal Rodinia in the Tonian true polar wander frame. *Earth and Planetary Science Letters*, **530**, 115880, https://doi.org/10.1016/j.epsl.2019.115880

Johnson, T.E., Kirkland, C.L., Gardiner, N.J., Brown, M., Smithies, R.H. and Santosh, M. 2019. Secular change in TTG compositions: Implications for the evolution of Archaean geodynamics. *Earth and Planetary Science Letters*, **505**, 66–75, https://doi.org/10.1016/j.epsl.2018.10.022

Jones, S.A., Cassidy, K.F. and Davis, B.K. 2020. Unravelling the D_1 event: evidence for early granite-up, greenstone-down tectonics in the Eastern Goldfields, Western Australia. *Australian Journal of Earth Sciences*, **68**, 1–35, https://doi.org/10.1080/08120099.2020.1755364

Kah, L.C., Bartley, J.K. and Teal, D.A. 2012. Chemostratigraphy of the Late Mesoproterozoic Atar Group, Taoudeni Basin, Mauritania: Muted isotopic variability, facies correlation, and global isotopic trends. *Precambrian Research*, **200–203**, 82–103, https://doi.org/10.1016/j.precamres.2012.01.011

Kamber, B.S. and Tomlinson, E.L. 2019. Petrological, mineralogical and geochemical peculiarities of Archean cratons. *Chemical Geology*, **511**, 123–151, https://doi.org/10.1016/j.chemgeo.2019.02.011

Karhu, J. and Holland, H.D. 1996. Carbon isotopes and the rise of atmospheric oxygen. *Geology*, **24**, 867–870, https://doi.org/10.1130/0091-7613(1996)024<0867:CIATRO>2.3.CO;2

Kaufman, A.J., Knoll, A.H. and Narbonne, G.M. 1997. Isotopes, ice ages, and terminal Proterozoic Earth history. *Proceedings of the National Academy of Sciences*, **95**, 6600–6605, https://doi.org/10.1073/pnas.94.13.6600

Kennedy, M.J., Runnegar, B., Prave, A.R., Hoffmann, K.H. and Arthur, M. 1998. Two or four Neoproterozoic glaciations? *Geology*, **26**, 1059–1063, https://doi.org/10.1130/0091-7613(1998)026<1059:TOFNG>2.3.CO;2

Kipp, M.A., Stüeken, E.E., Bekker, A. and Buick, R. 2017. Selenium isotopes record extensive marine suboxia during the Great Oxidation Event. *Proceedings of the National Academy of Sciences*, **114**, 875–880, https://doi.org/10.1073/pnas.1615867114

Kipp, M.A., Lepland, A. and Buick, R. 2020. Redox fluctuations, trace metal enrichment and phosphogenesis in the *c.* 2.0 Ga Zaonega Formation. *Precambrian Research*, **343**, 105716, https://doi.org/10.1016/j.precamres.2020.105716

Kirscher, U., Liu, Y., Li, Z.X., Mitchell, R.N., Pisarevsky, S., Denyszyn, S.W. and Nordsvan, A. 2019. Paleomagnetism of the Hart Dolerite (Kimberley, Western Australia) - A two-stage assembly of the supercontinent Nuna? *Precambrian Research*, **329**, 170–181, https://doi.org/10.1016/j.precamres.2018.12.026

Kirscher, U., Mitchell, R.N. *et al.* 2021. Paleomagnetic constraints on the duration of the Australia-Laurentia connection in the core of the Nuna supercontinent. *Geology*, **49**, 174–179, https://doi.org/10.1130/G47823.1

Klein, C. 2005. Some Precambrian banded iron-formations (BIFs) from around the world: Their age, geologic setting, mineralogy, metamorphism, geochemistry, and origin. *American Mineralogist*, **90**, 1473–1499, https://doi.org/10.2138/am.2005.1871

Knoll, A.H. 2000. Learning to tell Neoproterozoic time. *Precambrian Research*, **100**, 3–20, https://doi.org/10.1016/S0301-9268(99)00067-4

Knoll, A., Kaufman, A. and Semikhatov, M. 1995. The carbon-isotopic composition of Proterozoic carbonates: Riphean successions from northwestern Siberia (Anabar Massif, Turukhansk Uplift). *American Journal of Science*, **295**, 823–850, https://doi.org/10.2475/ajs.295.7.823

Knoll, A., Walter, M. and Christie-Blick, N. 2004. A new period for the geological time scale. *Science*, **305**, 621–622, https://doi.org/10.1126/science.1098803

Knoll, A.H., Javaux, E.J., Hewitt, D. and Cohen, P. 2006*a*. Eukaryotic organisms in Proterozoic oceans. *Philosophical Transactions of the Royal Society B*, **361**, 1023–1038, https://doi.org/10.1098/rstb.2006.1843

Knoll, A.H., Walter, M.R., Narbonne, G.M. and Christie-Blick, N. 2006*b*. The Ediacaran Period: a new addition to the geologic time scale. *Lethaia*, **39**, 13–30, https://doi.org/10.1080/00241160500409223

Kulling, O. 1934. The Hecla Hoek Formation around Hinlopenstredet. *Geografiska Annaler*, **14**, 161–253, https://doi.org/10.1080/20014422.1934.11880584

Kump, L.R., Junium, C. *et al.* 2011. Isotopic evidence for massive oxidation of organic matter following the great oxidation event. *Science*, **334**, 1694–1696, https://doi.org/10.1126/science.1213999

Kunzmann, M., Schmid, S., Blaikie, T.N. and Halverson, G.P. 2019. Facies analysis, sequence stratigraphy, and carbon isotope chemostratigraphy of a classic Zn–Pb host succession: The Proterozoic middle McArthur Group, McArthur Basin, Australia. *Ore Geology Reviews*, **106**, 150–175, https://doi.org/10.1016/j.oregeorev.2019.01.011

Kuznetsov, A.B., Semikhatov, M.A., Maslov, A.V., Gorokhov, I.M., Prasolov, E.M., Krupenin, M.T. and Kislova, I.V. 2006. New data on Sr- and C-isotopic chemostratigraphy of the Upper Riphean type section (southern Urals). *Stratigraphy and Geological Correlation*, **14**, 602–628, https://doi.org/10.1134/S0869593806060025

Kuznetsov, A.B., Melezhik, V.A., Gorokhov, I.M., Melnikov, N.N., Konstantinova, G.V., Kutyavin, E.P. and Turchenko, T.L. 2010. Sr isotopic composition of Paleoproterozoic 13C-rich carbonate rocks: the Tulomozero Formation, SE Fennoscandian Shield. *Precambrian Research*, **182**, 300–312, https://doi.org/10.1016/j.precamres.2010.05.006

Kuznetsov, A.B., Bekker, A., Ovchinnikova, G.V., Gorokhov, I.M. and Vasilyeva, I.M. 2017. Unradiogenic strontium and moderate-amplitude carbon isotope variations in early Tonian seawater after the assembly of Rodinia and before the Bitter Springs Excursion. *Precambrian Research*, **298**, 157–173, https://doi.org/10.1016/j.precamres.2017.06.011

Kuznetsov, A.B., Semikhatov, M.A. and Gorokhov, I.M. 2018. Strontium isotope stratigraphy: principles and state-of-the-art. *Stratigraphy and Geological Correlation*, **26**, 367–386, https://doi.org/10.1134/S0869593818040056

Lantink, M.L., Davies, J.H.F.L., Mason, P.R.D., Schaltegger, U. and Hilgen, F.J. 2019. Climate control on banded iron formations linked to orbital eccentricity. *Nature Geoscience*, **12**, 369–374, https://doi.org/10.1038/s41561-019-0332-8

Lee, Y.Y. 1936. The Sinian glaciation in the lower Yangtze Valley. *Bulletin of the Geoogical Society of China*, **15**, 131–134, https://doi.org/10.1111/j.1755-6724.1936.mp15001010.x

Lepot, K., Addad, A., Knoll, A.H., Wang, J., Troadac, D., Beché, A. and Javaux, E. 2017. Iron minerals within specific microfossil morphospecies of the 1.88 Ga Gunflint Formation. *Nature Communications*, **8**, 14890, https://doi.org/10.1038/ncomms14890

Li, Z.X., Li, X.H., Kinny, P.D. and Wang, J. 1999. The breakup of Rodinia: did it start with a mantle plume beneath South China? *Earth and Planetary Science Letters*, **173**, 171–181. https://doi.org/10.1016/S0012-821X(99)00240-X

Li, Z.X., Evans, D.A.D. and Zhang, S. 2004. A 90° spin on Rodinia: possible causal links between the Neoproterozoic supercontinent, superplume, true polar wander and low-latitude glaciation. *Earth and Planetary Science Letters*, **220**, 409–421, https://doi.org/10.1016/S0012-821X(04)00064-0

Li, Z.X., Evans, D.A.D. and Halverson, G.P. 2013. Neoproterozoic glaciations in a revised global palaeogeography from the breakup of Rodinia to the assembly of Gondwanaland. *Sedimentary Geology*, **294**, 219–232, https://doi.org/10.1016/j.sedgeo.2013.05.016

Lindsay, J.F. 1987. Upper Proterozoic evaporites in the Amadeus basin, central Australia, and their role in basin tectonics. *Geological Society of America Bulletin*, **99**, 852–865, https://doi.org/10.1130/0016-7606(1987)99<852:UPEITA>2.0.CO;2

Lindsay, J.F. 2002. Supersequences, superbasins, supercontinents–evidence from the Neoproterozoic–Early Palaeozoic basins of central Australia. *Basin Research*, **14**, 207–223, https://doi.org/10.1046/j.1365-2117.2002.00170.x

Lindsay, J.F. and Brasier, M.D. 2002. Did global tectonics drive early biosphere evolution? Carbon isotope record from 2.6 to 1.9 Ga carbonates of Western Australian basins. *Precambrian Research*, **114**, 1–34, https://doi.org/10.1016/S0301-9268(01)00219-4

Liu, Y., Mitchell, R.N., Li, Z.X., Kirscher, U., Pisarevsky, S. and Wang, C. 2021. Archean geodynamics: Ephemeral supercontinents or long-lived supercratons. *Geology*, https://doi.org/10.1130/G48575.1

Logan, W.E. 1857. On the division of Azoic rocks of Canada into Huronian and Laurentian. *Proceedings of the American Association for the Advancement of Science*, **1857**, 44–47.

Loron, C. and Moczydłowska, M. 2017. Tonian (Neoproterozoic) eukaryotic and prokaryotic organic-walled microfossils from the upper Visingsö Group, Sweden. *Palynology*, **42**, 220–254, https://doi.org/10.1080/01916122.2017.1335656

Loron, C.C., Rainbird, R.H., Turner, E.C., Greenman, J.W. and Javaux, E.J. 2019*a*. Organic-walled microfossils from the late Mesoproterozoic to early Neoproterozoic lower Shaler Supergroup (Arctic Canada): diversity and biostratigraphic significance. *Precambrian Research*, **321**, 349–374, https://doi.org/10.1016/j.precamres.2018.12.024

Loron, C.C., François, C., Rainbird, R.H., Turner, E.C., Borensztajn, S. and Javaux, E.J. 2019*b*. Early fungi from the Proterozoic Era in Arctic Canada. *Nature*, **270**, 232–235, https://doi.org/10.1038/s41586-019-1217-0

Luo, G., Ono, S., Beukes, N.J., Wang, D.T., Xie, S. and Summons, R.E. 2016. Rapid oxygenation of Earth's atmosphere 2.33 billion years ago. *Scientific Advances*, **2**, e1600134, https://doi.org/10.1126/sciadv.1600134

Macdonald, F.A. and Wordsworth, R. 2017. Initiation of Snowball Earth with volcanic sulfur aerosol emissions. *Geophysical Research Letters*, **44**, 1938–1946, https://doi.org/10.1002/2016GL072335

Macdonald, F.A., Schmitz, M.D. *et al.* 2010. Calibrating the Cryogenian. *Science*, **327**, 1241–1243, https://doi.org/10.1126/science.1183325

Macdonald, F.A., Halverson, G.P., Strauss, J., Smith, E., Cox, G. and Sperling, E. 2012. Early Neoproterozoic basin formation in Yukon, Canada: Implications for the make-up and break-up of Rodinia. *Geoscience Canada*, **39**, 77–100.

Macdonald, F.A., Schmitz, M.D. *et al.* 2018. Cryogenian of Yukon. *Precambrian Research*, **319**, 114–143, https://doi.org/10.1016/j.precamres.2017.08.015

MacLennan, S., Park, Y. *et al.* 2018. The arc of the Snowball: U–Pb dates constrain the Islay anomaly and the initiation of the Sturtian glaciation. *Geology*, **46**, 539–542, https://doi.org/10.1130/G40171.1

Manhes, G., Allègre, C., Dupré, C. and Hamelin, B. 1980. Lead isotope study of basic-ultrabasic layered complexes: Speculations about the age of the earth and primitive mantle characteristics. *Earth and Planetary Science Letters*, **47**, 370–382, https://doi.org/10.1016/0012-821X(80)90024-2

Martin, A.P., Condon, D.J., Prave, A.R. and Lepland, A. 2013. A review of temporal constraints for the Palaeoproterozoic large, positive carbonate carbon isotope excursion (the Lomagundi-Jatuli Event. *Earth Science Reviews*, **127**, 242–261, https://doi.org/10.1016/j.earscirev.2013.10.006

Martin, A.P., Prave, A.R. *et al.* 2015. Multiple Palaeoproterozoic carbon burial episodes and excursions. *Earth and Planetary Science Letters*, **424**, 226–236, https://doi.org/10.1016/j.epsl.2015.05.023

Mawson, D. 1949. The Late Precambrian ice age and glacial record of the Bibliando dome. *Journal and Proceedings of the Royal Society of New South Wales*, **82**, 150–174.

McArthur, J.M., Howarth, R.J., Shields, G.A. and Zhou, Y. 2020. Strontium isotope stratigraphy. *In*: Gradstein, F.M., Ogg, J.G., Schmitz, M.D. and Ogg, G.M. (eds) *The Geologic Time Scale 2020*. Elsevier Science, **1**, 211–238.

McKenzie, R.N., Hughes, N.C., Myrow, P.M., Banerjee, D.M., Deb, M. and Planavasky, N.J. 2013. New age constraints for the Proterozoic-Delhi successions of India and their implications. *Precambrian Research*, **238**, 120–128, https://doi.org/10.1016/j.precamres.2013.10.006

McLelland, J.M., Selleck, B.W., Hamilton, M.A. and Bickford, M.E. 2010. Late- to post-tectonic setting of some major Proterozoic anorthosite-mangerite-charnokite-granite (AMCG) suites. *Canadian Mineralogist*, **48**, 729–750, https://doi.org/10.3749/canmin.48.4.729

Melezhik, V.A., Filippov, M.M. and Romaskin, A.E. 2004. A giant Palaeoproterozoic deposit of shungite in NW Russia: Genesis and practical applications. *Ore Geology Reviews*, **24**, 135–154, https://doi.org/10.1016/j.oregeorev.2003.08.003

Melezhik, V.A., Fallick, A.E., Hanski, E.J., Kump, L.R., Lepland, A., Prave, A.R. and Strauss, H. 2005. Emergence of the aerobic biosphere during the Archean–Proterozoic transition: Challenges of future research. *GSA Today*, **15**, 4–11, https://doi.org/10.1130/1052-5173(2005)015[4:EOAABD]2.0.CO;2

Melezhik, V.A., Huhma, H., Condon, D.J., Fallick, A.E. and Whitehouse, M.J. 2007. Temporal constraints on the Paleoproterozoic Lomagundi-Jatuli carbon isotopic event. *Geology*, **35**, 655–658, https://doi.org/10.1130/G23764A.1

Meng, Q., Wei, H., Qu, Y. and Ma, S. 2011. Stratigraphic and sedimentary records of the rift to drift evolution of the northern North China craton at the Paleo- to Mesoproterozoic transition. *Gondwana Research*, **20**, 205–218, https://doi.org/10.1016/j.gr.2010.12.010

Merdith, A.S., Collins, A.S. *et al.* 2017*a*. A full-plate global reconstruction of the Neoproterozoic. *Gondwana Research*, **50**, 84–134, https://doi.org/10.1016/j.gr.2017.04.001

Merdith, A.S., Williams, S.E., Müller, R.D. and Collins, A.S. 2017*b*. Kinematic constraints on the Rodinia to Gondwana transition. *Precambrian Research*, **299**, 132–150, https://doi.org/10.1016/j.precamres.2017.07.013

Merdith, A.S., Williams, S.E., Brune, S., Collins, A.S. and Müller, R.D. 2019. Rift and plate boundary evolution across two supercontinent cycles. *Global and Planetary Change*, **173**, 1–14, https://doi.org/10.1016/j.gloplacha.2018.11.006

Miao, L., Moczydłowska, M., Zhu, S. and Zhu, M. 2019. New record of organic-walled, morphologically distinct microfossils from the late Paleoproterozoic Changcheng Group in the Yanshan Range, North China. *Precambrian Research*, **321**, 172–198, https://doi.org/10.1016/j.precamres.2018.11.019

Mitchell, R.N. 2014. True polar wander and supercontinent cycles: implications for lithospheric elasticity an d the triaxial earth. *American Journal of Science*, **514**, 966–979, https://doi.org/10.2475/05.2014.04

Mitchell, R.N., Kilian, T.M. and Evans, D.A.D. 2012. Supercontinent cycles and the calculation of absolute palaeolongitude in deep time. *Nature*, **482**, 208–211, https://doi.org/10.1038/nature10800

Mitchell, R.N., Zhang, N. *et al.* 2021. The supercontinent cycle. *Nature Reviews: Earth and environment*, https://doi.org/10.1038/s43017-021-00160-0

Moreira, H., Seixas, L., Storey, C., Fowler, M., Lasalle, S., Stevenson, R. and Lana, C. 2018. Evolution of Siderian juvenile crust to Rhyacian high Ba-Sr magmatism in the Mineiro Belt, southern São Francisco Craton. *Geoscience Frontiers*, **9**, 977–995, https://doi.org/10.1016/j.gsf.2018.01.009

Nagovitsin, K. 2009. *Tappania*-bearing association of the Siberian platform: Biodiversity, stratigraphic position and geochronological constraints. *Precambrian Research*, **173**, 137–145, https://doi.org/10.1016/j.precamres.2009.02.005

Nance, R.D. and Murphy, J.B. 2018. Supercontinents and the case for Pannotia. *Geological Society, London, Special Publications*, **470**, 65–86, https://doi.org/10.1144/SP470.5

Nance, R.D., Worsley, T.R. and Moody, J.B. 1986. Post-Archean biogeochemical cycles and long-term episodicity in tectonic processes. *Geology*, **14**, 514–518, https://doi.org/10.1130/0091-7613(1986)14<514:PBCALE>2.0.CO;2

Nelson, L.L., Smith, E.F., Hodgin, E.B., Crowley, J.L., Schmitz, M.D. and Macdonald, F.A. 2020. Geochronological constraints on Neoproterozoic rifting and onset of the Marinoan glaciation from the Kingston Peak Formation in Death Valley, California (USA). *Geology*, **48**. https://doi.org/10.1130/G47668.1

Nutman, A.P., McGregor, V.R., Friend, C.R.L., Bennett, V.C. and Kinny, P.D. 1996. The Itsaq Gneiss Complex of southern West Greenland; the world's most extensive record of early crustal evolution (3900–3600 Ma). *Precambrian Research*, **78**, 1–39, https://doi.org/10.1016/0301-9268(95)00066-6

Och, L.M. and Shields-Zhou, G.A. 2012. The Neoproterozoic oxygenation event: Environmental perturbations and biogeochemical cycling. *Earth Science Reviews*, **110**, 26–57, https://doi.org/10.1016/j.earscirev.2011.09.004

O'Neill, C., Lenardic, A. and Condie, K.C. 2015. Earth's punctuated tectonic evolution: cause and effect. *Geological Society, London, Special Publications*, **389**, 17–40, https://doi.org/10.1144/SP389.4

Ossa Ossa, F., Hofmann, A. *et al.* 2019. Limited oxygen production in the Mesoarchean ocean. *Proceedings of the National Academy of Sciences*, **116**, 6647–6652, https://doi.org/10.1073/pnas.1818762116

Ostrander, C.M., Nielsen, S.G., Owens, J.G., Kendall, B., Gordon, G.W., Romaniello, S.J. and Anbar, A.D. 2019. Fully oxygenated water columns over continental shelves before the Great Oxidation Event. *Nature Geoscience*, **12**, 186–191, https://doi.org/10.1038/s41561-019-0309-7

Ouyang, G., She, Z., Papineau, D., Wang, X., Luo, G. and Li, C. 2020. Dynamic carbon and sulfur cycling in the aftermath of the Lomagundi-Jatuli Event: Evidence from the Paleoproterozoic Hutuo Supergroup, North China Craton. *Precambrian Research*, **337**, 105549, https://doi.org/10.1016/j.precamres.2019.105549

Pang, K., Tang, Q., Wan, B. and Yuan, X. 2020. New insights on the palaeobiology and biostratigraphy of the acritarch *Trachyhystrichosphaera aimika*: a potential late Mesoproterozoic to Tonian index fossil. *Palaeoworld*, https://doi.org/10.1016/j.palwor.2020.02.003

Parfrey, L.W., Lahr, D.J.G., Knoll, A.H. and Katz, L.A. 2011. Estimating the timing of early eukaryotic diversification with multigene molecular clocks. *Proceedings of the National Academy of Sciences*, **108**, 13624–13629, https://doi.org/10.1073/pnas.1110633108

Park, H.U., Zhai, J.H. *et al.* 2016. Deposition age of the Sangwon Supergroup in the Pyongnam basin (Korea) and the early Tonian negative carbon isotope interval. *Acta Petrologica Sinica*, **32**, 2181–2195.

Partin, C.A., Bekker, A. *et al.* 2013. Large-scale fluctuations in Precambrian atmospheric and oceanic oxygen levels from the record of U in shales. *Earth and Planetary Science Letters*, **369**, 284–293, https://doi.org/10.1016/j.epsl.2013.03.031

Partin, C.A., Bekker, A., Sylvester, P.J., Wodicka, N., Stern, R.A., Chacko, T. and Heaman, L.M. 2014. Filling the juvenile magmatic gap: Evidence of uninterrupted Paleoproterozoic plate tectonics. *Earth and Planetary Science Letters*, **388**, 123–124, https://doi.org/10.1016/j.epsl.2013.11.041

Patterson, C. 1956. Age of meteorites and the Earth. *Geochimica et Cosmochimica Acta*, **10**, 230–237, https://doi.org/10.1016/0016-7037(56)90036-9

Payne, J.L., Hand, M., Barovich, K.M., Reid, A. and Evans, D.A.D. 2009. Correlations and reconstruction models for the 2500–1500 Ma evolution of the Mawson Continent. *Geological Society, London, Special Publications*, **323**, 319–355, https://doi.org/10.1144/SP323.16

Peng, P. 2015. Precambrian mafic dyke swarms in the North China Craton and their geological implications. *Science China Earth Sciences*, **58**, 649–675, https://doi.org/10.1007/s11430-014-5026-x

Peng, S.C., Babcock, L.E. and Ahlberg, P. 2020. The Cambrian Period. *In*: Gradstein, F.M., Ogg, J.G., Schmitz, M. and Ogg, G. (eds) *The Geologic Time Scale 2020*. Elsevier Science, **2**, 565–629.

Philippot, P., Avila, J.N. *et al.* 2018. Globally asynchronous Sulphur isotope signals require re-definition of the Great Oxidation Event. *Nature Communications*, **9**, 1–10, https://doi.org/10.1038/s41467-018-04621-x

Pietrzak-Renaud, N. and Davis, D. 2014. U–Pb geochronology of baddeleyite from the Belleview metadiabase: Age and geotectonic implications for the Negaunee Iron Formation, Michigan. *Precambrian Research*, **250**, 1–5, https://doi.org/10.1016/j.precamres.2014.05.018

Pisarevsky, S.A., Elming, S-Å, Pesonen, L.J. and Li, Z.-X. 2014. Mesoproterozoic paleogeography: Supercontinent and beyond. *Precambrian Research*, **244**, 207–225, https://doi.org/10.1016/j.precamres.2013.05.014

Planavsky, N., Rouxel, O., Bekker, A., Shapiro, R., Fralick, P. and Knudsen, A. 2009. Iron-oxidizing microbial ecosystems thrived in late Paleoproterozoic redox-stratified oceans. *Earth and Planetary Science Letters*, **286**, 230–242, https://doi.org/10.1016/j.epsl.2009.06.033

Plumb, K.A. 1991. New Precambrian time scale. *Episodes*, **14**, 139–140, https://doi.org/10.18814/epiiugs/1991/v14i2/005

Plumb, K.A. 1992. New Precambrian time scale – reply. *Episodes*, **15**, 124–125, https://doi.org/10.18814/epiiugs/1992/v15i2/006

Plumb, K.A. and James, H.L. 1986. Subdivision of Precambrian time: recommendations and suggestions by Subcommission on Precambrian stratigraphy. *Precambrian Research*, **32**, 65–92, https://doi.org/10.1016/0301-9268(86)90031-8

Porter, S.M. 2016. Tiny vampires in ancient seas: evidence for predation via perforation in fossils from the 780–740 million-year-old Chuar Group, Grand Canyon, USA. *Proceedings of the Royal Society B*, **283**, 20160221, https://doi.org/10.1098/rspb.2016.0221

Porter, S.M. and Knoll, A.H. 2000. Testate amoebae in the Neoproterozoic Era: evidence from vase-shaped microfossils in the Chuar Group, Grand Canyon. *Paleobiology*, **26**, 360–385, https://doi.org/10.1666/0094-8373(2000)026<0360:TAITNE>2.0.CO;2

Porter, S.M., Meisterfeld, R. and Knoll, A.H. 2003. Vase-shaped microfossils from the Neoproterozoic Chuar Group, Grand Canyon: a classification guided by modern testate amoebae. *Journal of Paleontology*, **77**, 409–429, https://doi.org/10.1666/0022-3360(2003)077<0409:VMFTNC>2.0.CO;2

Poulton, S.W. and Canfield, D.E. 2011. Ferruginous conditions: A dominant feature of oceans throughout Earth's history. *Elements*, **7**, 107–112, https://doi.org/10.2113/gselements.7.2.107

Poulton, S.W., Fralick, P.W. and Canfield, D.E. 2004. The transition to a sulphidic ocean approximately 1.84 billion years ago. *Nature*, **431**, 173–177, https://doi.org/10.1038/nature02912

Poulton, S.W., Fralick, P.W. and Canfield, D.E. 2010. Spatial variability in oceanic redox structure 1.8 billion years ago. *Nature Geoscience*, **3**, 486–490, https://doi.org/10.1038/ngeo889

Poulton, S.W., Bekker, A., Cumming, V.M., Zerkle, A.L., Canfield, D.E. and Johnston, D.T. 2021. A 200-million-year delay in permanent atmospheric oxygenation. *Nature*, https://doi.org/10.1038/s41586-021-03393-7

Pourteau, A., Smit, M.A., Li, Z.X., Collins, W.J., Nordsvan, A.R., Volante, S. and Li, J. 2018. 1.6 Ga crustal thickening along the final Nuna suture. *Geology*, **46**, 959–962, https://doi.org/10.1130/G45198.1

Prave, A.R., Condon, D.J., Hoffmann, K.H., Tapster, S. and Fallick, A.E. 2016. Duration and nature of the end-Cryogenian (Marinoan) glaciation. *Geology*, **44**, 631–634, https://doi.org/10.1130/G38089.1

Prince, J.K.G., Rainbird, R.H. and Wing, B.A. 2019. Evaporite deposition in the mid-Neoproterozoic as a driver for changes in seawater chemistry and the biogeochemical cycle of sulfur. *Geology*, **47**, 291–294, https://doi.org/10.1130/G45413.1

Puchkov, V.N., Krasnobaev, A.A. and Sergeeva, N.D. 2014. The new data on stratigraphy of the Riphean Stratotype in the Southern Urals, Russia. *Journal of Geoscience and Environment Protection*, **2**, 108–116, https://doi.org/10.4236/gep.2014.23015

Puetz, S.J. and Condie, K. 2019. Time series analysis of mantle cycles Part 1: Periodicities and correlations among seven global isotopic databases. *Geoscience Frontiers*, **10**, 1305–1326, https://doi.org/10.1016/j.gsf.2019.04.002

Qu, Y., Pan, J., Ma, S., Lei, Z., Li, L. and Wu, G. 2014. Geological characteristics and tectonic significance of unconformities in Mesoproterozoic successions in the northern margin of the North China Block. *Geoscience Frontiers*, **5**, 127–138, https://doi.org/10.1016/j.gsf.2013.04.002

Rainbird, R.H., Jefferson, C.W. and Young, G.M. 1996. The early Neoproterozoic sedimentary succession B of northwestern Laurentia: Correlations and paleogeographic significance. *Geological Society of America Bulletin*, **108**, 454–470, https://doi.org/10.1130/0016-7606(1996)108<0454:TENSSB>2.3.CO;2

Ranjan, S., Upadhyay, D., Pruseth, K.L. and Nanda, J.K. 2020. Detrital zircon evidence for change in geodynamic regime of continental crust formation 3.7–3.6 billion years ago. *Earth and Planetary Science Letters*, **538**, 116206, https://doi.org/10.1016/j.epsl.2020.116206

Rawlings, D.J. 1999. Stratigraphic resolution of a multiphase intracratonic basin system: the McArthur Basin, northern Australia. *Australian Journal of Earth Sciences*, **46**, 703–723, https://doi.org/10.1046/j.1440-0952.1999.00739.x

Ray, J.S. 2006. Age of the Vindhyan Supergroup: A review of recent findings. *Journal of Earth System Science*, **115**, 149–160, https://doi.org/10.1007/BF02703031

Reusch, H. 1891. Skuringmærker og morængus eftervist i Finnmarken fra en periode meget ældre end 'istiden' [Glacial striae and boulder-clay in Norwegian Lapponie from a period much older than the last ice age]. *Norges Geologiske Undersøkelse*, 1, **78–85**, 97–100.

Rice, A.H.N., Edwards, M.B., Hansen, T.A., Arnaud, E. and Halverson, G.P. 2011. Glaciogenic rocks of the Neoproterozoic Smalfjord and Mortenses formations, Verstertana Group, E. Finnmark, Norway. Geological Society, London, Memoirs, **36**, 593–602, https://doi.org/10.1144/M36.57

Riding, R. 2008. Abiogenic, microbial and hybrid authigenic carbonate crusts: components of Precambrian stromatolites. *Geologica Croatia*, **61**, 73–103.

Riding, R. 2011. The nature of stromatolites: 3,500 million years of history and a century of research. *In*: Reitner, J., Queric, N.-V. and Arp, G. (eds) *Advances in Stromatolite Geobiology*. Lecture Notes in Earth Sciences, **131**, 29–74, https://doi.org/10.1007/978-3-642-10415-2_3

Riding, R., Fralick, P. and Liang, L. 2014. Identification of an Archean marine oxygen oasis. *Precambrian Research*, **251**, 232–237, https://doi.org/10.1016/j.precamres.2014.06.017

Riedman, L.A. and Sadler, P.M. 2018. Global species richness record and biostratigraphic potential of early to middle Neoproterozoic eukaryote fossils. *Precambrian Research*, **319**, 6–18, https://doi.org/10.1016/j.precamres.2017.10.008

Riedman, L.A., Porter, S.M. and Calver, C.R. 2018. Vase-shaped microfossil biostratigraphy with new data from Tasmania, Svalbard, Greenland, Sweden and the Yukon. *Precambrian Research*, **319**, 19–36, https://doi.org/10.1016/j.precamres.2017.09.019

Rivers, T. 2015. Tectonic setting and evolution of the Grenville Orogen: An assessment of progress over the last 40 years. *Geoscience Canada*, **42**, 77–124, https://doi.org/10.12789/geocanj.2014.41.057

Robb, L.J., Knoll, A.H., Plumb, K.A., Shields, G.A., Strauss, H. and Veizer, J. 2004. The Precambrian: The Archean and Proterozoic Eons. *In*: Gradstein, F.M., Ogg, J.G. and Smith, A.G. (eds) *A Geologic Time Scale 2004*. Cambridge University Press, Cambridge, 129–140.

Rogers, J.J.W. and Santosh, M. 2002. Configuration of Columbia: a Mesoproterozoic supercontinent. *Gondwana Research*, **5**, 5–22, https://doi.org/10.1016/S1342-937X(05)70883-2

Rooney, A.D., Strauss, J.V., Brandon, A.D. and Macdonald, F.A. 2015. A Cryogenian chronology: Two long-lasting synchronous Neoproterozoic glaciations. *Geology*, **43**, 459–462, https://doi.org/10.1130/G36511.1

Rooney, A.D., Yang, C., Condon, D.J., Zhu, M. and Macdonald, F.A. 2020. U–Pb and Re-Os geochronology tracks stratigraphic condensation in the Sturtian snowball Earth aftermath. *Geology*, **48**, 625–629, https://doi.org/10.1130/G47246.1

Ross, G.M. and Villeneuve, M. 2003. Provenance of the Mesoproterozoic (1.45 Ga) Belt basin (western North America): another piece in the pre-Rodinia paleogeographic puzzle. *Geological Society of America Bulletin*, **115**, 1191–1217, https://doi.org/10.1130/B25209.1

Safonova, L. and Maruyama, S. 2014. Asia: a frontier for a future supercontinent Amasia. *International Geology Reviews*, **56**, 1051–1071, https://doi.org/10.1080/00206814.2014.915586

Sánchez-Baracaldo, P., Raven, J.A., Pisani, D. and Knoll, A.H. 2017. Early photosynthetic eukaryotes inhabited low-salinity habitats. *Proceedings of the National Academy of Sciences*, **114**, E7737–E7745, https://doi.org/10.1073/pnas.1620089114

Satkoski, A.M., Lowe, D.R., Beard, B.L., Coleman, M.L. and Johnson, C.M. 2016. A high continental weathering flux into Paleoarchean seawater revealed by strontium isotope analysis of 3.26 Ga barite. *Earth and Planetary Science Letters*, **454**, 28–35, https://doi.org/10.1016/j.epsl.2016.08.032

Schneider, D.A., Bickford, M.E., Cannon, W.F., Schulz, K.J. and Hamilton, M.A. 2002. Age of volcanic rocks and syndepositional iron formations, Marquette Range Supergroup: implications for the tectonic setting of Paleoproterozoic iron formations of the Lake Superior region. *Canadian Journal of Earth Sciences*, **39**, 999–1012, https://doi.org/10.1139/e02-016

Schroeder, S., Bekker, A., Beukes, N.J., Strauss, H. and van Niekerk, H.S. 2008. Rise in seawater sulphate concentrations associated with the Paleoproterozoic positive carbon isotope excursion: evidence from sulphate evaporites in the *c.* 2.2–2.1 Gyr shallow-marine Lucknow Formation, South Africa. *Terra Nova*, **20**, 108–117, https://doi.org/10.1111/j.1365-3121.2008.00795.x

Scott, C., Lyons, T.W., Bekker, A., Shen, Y.A., Poulton, S.W., Chu, X.L. and Anbar, A.D. 2008. Tracing the stepwise oxygenation of the Proterozoic ocean. *Nature*, **452**, 456–459, https://doi.org/10.1038/nature06811

Sedgwick, A. 1845. On the Older Palæozoic (Protozoic) Rocks of North Wales. *Quarterly Journal of the Geological Society*, **1**, 5–22, https://doi.org/10.1144/GSL.JGS.1845.001.01.02

Semikhatov, M.A., Kuznetsov, A.B. and Chumakov, N.M. 2015. Isotope age boundaries between the general stratigraphic subdivisions of the upper Proterozoic (Riphean and Vendian) in Russia: The evolution of opinions and the current estimate. *Stratigraphy and Geological Correlation*, **23**, 568–579, https://doi.org/10.1134/S0869593815060088

Sergeev, V.N., Vorob'eva, N.G. and Petrov, P.Y. 2017. The biostratigraphic conundrum of Siberia: do true Tonian–Cryogenian microfossils occur in Mesoproterozoic rocks? *Precambrian Research*, **299**, 282–302, https://doi.org/10.1016/j.precamres.2017.07.024

Shang, M., Tang, D., Shi, X., Zhou, L., Zhou, X., Song, H. and Jiang, G. 2019. A pulse of oxygen increase in the early Mesoproterozoic ocean at ca. 1.57–1.56 Ga. *Earth and Planetary Science Letters*, **527**, 115797, https://doi.org/10.1016/j.epsl.2019.115797

Sharma, M. and Shukla, Y. 2009. Taxonomy and affinity of Early Mesoproterozoic megascopically helically coiled and related fossils from the Rohtas Formation, the Vindhyan Supergroup, India. *Precambrian Research*, **173**, 105–122, https://doi.org/10.1016/j.precamres.2009.05.002

Shields, G.A. 2002. 'Molar-tooth microspar': a chemical explanation for its disappearance *c.* 750 Ma. *Terra Nova*, **14**, 108–113, https://doi.org/10.1046/j.1365-3121.2002.00396.x

Shields, G.A. 2007. A normalised seawater strontium isotope curve: possible implications for Neoproterozoic–Cambrian weathering rates and the further oxygenation of the Earth. *eEarth*, **2**, 35–42, https://doi.org/10.5194/ee-2-35-2007

Shields, G.A. 2017. Earth system transition during the Tonian–Cambrian interval of biological innovation: nutrients, climate, oxygen and the marine organic carbon capacitor. Geological Society, London. *Special Publications*, **448**, 161–177, https://doi.org/10.1144/SP448.17

Shields, G. and Veizer, J. 2002. Precambrian marine carbonate isotope database: Version 1.1. *Geochemistry Geophysics Geosystems*, **3**, 1–12, https://doi.org/10.1029/2001GC000266

Shields, G.A., Mills, B.J.W., Zhu, M., Daines, S. and Lenton, T.M. 2019. Unique Neoproterozoic carbon isotope excursions sustained by coupled evaporite dissolution and pyrite burial. *Nature Geoscience*, **12**, 823–827, https://doi.org/10.1038/s41561-019-0434-3

Shields-Zhou, G.A., Hill, A.C. and Macbabhann, B.A. 2012. The Cryogenian Period. Chapter 17. *In*: Gradstein, F.M., Ogg, J.G., Schmitz, M. and Ogg, G. (eds) *The Geological Time Scale 2012*. Elsevier, **1**, 393–411.

Shields-Zhou, G., Porter, S.A. and Halverson, G.P. 2016. A new rock-based definition for the Cryogenian Period (circa 720–635 Ma). *Episodes*, **39**, 3–9, https://doi.org/10.18814/epiiugs/2016/v39i1/89231

Shumlyanskyy, L., Ernst, R.E., Albekov, A., Söderlund, U., Wilde, S.A. and Bekker, A. 2021. The early Statherian (ca. 1800–1750Ma) Prutivka-Novogol large igneous province of Sarmatia: Geochronology and implication for the Nuna/Columbia supercontinent reconstruction. *Precambrian Research*, **358**, 106185, https://doi.org/10.1016/j.precamres.2021.106185

Singh, V.K., Sharma, M. and Sergeev, V.N. 2019. A New Record of Acanthomorphic Acritarch *Tappania* Yin from the Early Mesoproterozoic Saraipali Formation, Singhora Group, Chhattisgarh Supergroup, India and its Biostratigraphic Significance. *Journal of the Geological Society of India*, **94**, 471–479, https://doi.org/10.1007/s12594-019-1343-1

Sircombe, K.N., Bleeker, W. and Stern, R.A. 2001. Detrital zircon geochronology and grain-size analysis of a *c.* 2800 Ma Mesoarchean proto-cratonic succession, Slave Province, Canada. *Earth and Planetary Science Letters*, **189**, 207–220, https://doi.org/10.1016/S0012-821X(01)00363-6

Sossi, P.A., Eggins, S.M., *et al.* 2016. Petrogenesis and geochemistry of Archean komatiites. *Journal of Petrology*, **57**, 147–184, https://doi.org/10.1093/petrology/egw004

Spaggiari, C.V., Kirkland, C.L., Smithies, R.H., Wingate, M.T.D. and Belousova, E.A. 2015. Transformation of an Archean craton margin during Proterozoic basin formation and magmatism: The Albany-Fraser Orogen, Western Australia. *Precambrian Research*, **266**, 440–466, https://doi.org/10.1016/j.precamres.2015.05.036

Spencer, C.J. 2020. Continuous continental growth as constrained by the sedimentary record. *American Journal of Science*, **320**, 373–401, https://doi.org/10.2475/04.2020.02

Spencer, C.J., Hawkesworth, C., Cawood, P.A. and Dhuime, B. 2013. Not all supercontinents are created equal: Gondwana-Rodinia case study. *Geology*, **41**, 795–798, https://doi.org/10.1130/G34520.1

Spencer, C.J., Murphy, J.B., Kirkland, C.L., Liu, Y. and Mitchell, R.M. 2018. A Palaeoproterozoic tecton-magmatic lull as a potential trigger for the supercontinent cycle. *Nature Geoscience*, **11**, 97–101, https://doi.org/10.1038/s41561-017-0051-y

Sprigg, R.C. 1947. Early Cambrian (?) jellyfishes from the Flinders Ranges, South Australia. *Transactions of the Royal Society of South Australia*, **71**, 212–224.

Stern, R.A. and Bleeker, W. 1998. Age of the world's oldest rocks refined using Canada's SHRIMP: Acasta Gneiss Complex, Northwest Territories. *Geoscience Canada*, **25**, 27–31.

Stockwell, C.H. 1961. Structural provinces, orogenies, and time classification of rocks of the Canadian Precambrian Shield. *Geological Survey of Canada, Paper*, **61–17**, 108–118.

Stockwell, C.H. 1982. Proposals for time classification and correlation of Precambrian rocks and events in Canada and adjacent areas of the Canadian Shield. Part 1: A time classification of Precambrian rocks and events. *Geological Survey of Canada, Paper*, **80–19**.

Strachan, R., Murphy, J.B., Darling, J., Storey, C. and Shields, G.A. 2020. Precambrian (4.56–1.0 Ga). *In*: Gradstein, F.M., Ogg, J.G., Schmitz, M.D. and Ogg, G.M. (eds) *The Geologic Time Scale 2020*. Elsevier Science Limited, **1**, 481–493.

Strauss, J.V., Rooney, A.D., Macdonald, F.A., Brandon, A.D. and Knoll, A.H. 2014. 740 Ma vase-shaped microfossils from Yukon, Canada: implications for Neoproterozoic chronology and biostratigraphy. *Geology*, **42**, 659–662, https://doi.org/10.1130/G35736.1

Swanson-Hysell, N.L., Maloof, A.C., Kirschvink, J.L., Evans, D.A.D., Halverson, G.P. and Hurtgen, M.T. 2012. Constraints on Neoproterozoic paleogeography and Paleozoic orogenesis from paleomagnetic records of the Bitter Springs Formation, central Australia. *American Journal of Science*, **312**, 817–884, https://doi.org/10.2475/08.2012.01

Swanson-Hysell, N.L., Maloof, A.C., *et al.* 2015. Stratigraphy and geochronology of the Tambien Group, Ethiopia: Evidence for globally synchronous carbon isotope change in the Neoproterozoic. *Geology*, **43**, 323–326, https://doi.org/10.1130/G36347.1

Tang, H. and Chen, Y. 2013. Global glaciations and atmospheric change at *c.* 2.3 Ga. *Geoscience Frontiers*, **4**, 583–596, https://doi.org/10.1016/j.gsf.2013.02.003

Tang, Q., Pang, K., Xiao, S., Yuan, X., Ou, Z. and Wan, B. 2013. Organic-walled microfossils from the early Neoproterozoic Liulaobei Formation in the Huainan region of North China and their biostratigraphic significance. *Precambrian Research*, **236**, 157–181, https://doi.org/10.1016/j.precamres.2013.07.019

Tang, Q., Pang, K., Yuan, X. and Xiao, S. 2020. A one-billion-year-old multicellular chlorophyte. *Nature Ecology & Evolution*, **4**, 543–549, https://doi.org/10.1038/s41559-020-1122-9

Tegner, C., Andersen, T.B., *et al.* 2019. A mantle plume origin for the Scandinavian Dyke Complex: A 'piercing point' for 615 Ma plate reconstruction of Baltica? *Geochemistry, Geophysics, Geosystems*, **20**, 1075–1094, https://doi.org/10.1029/2018GC007941

Teixeira, W., Geraldes, M.C., Matos, R., Salina Ruiz, A., Saes, G. and Vargas-Mattos, G. 2010. A review of the tectonic evolution of the Sunsas Belt, SW Amazonian craton. *Journal of South American Earth Sciences*, **29**, 47–60, https://doi.org/10.1016/j.jsames.2009.09.007

Thomson, J. 1871. *On the stratified rocks of Islay. Report of the 41st Meeting of the British Association for the Advancement of Science*. John Murray, London, 110–111.

Thomson, J. 1877. On the geology of the island of Islay. *Transactions of the Geological Society of Glasgow*, **5**, 200–222, https://doi.org/10.1144/transglas.5.2.200

Thomson, D., Rainbird, R.H., Planavsky, N., Lyons, T.W. and Bekker, A. 2015. Chemostratigraphy of the Shaler Supergroup, Victoria Island, NW Canada: a record of ocean composition prior to the Cryogenian glaciations. *Precambrian Research*, **263**, 232–245, https://doi.org/10.1016/j.precamres.2015.02.007

Trendall, A.F. 1966. Towards rationalism in Precambrian stratigraphy. *Journal of the Geological Society of Australia*, **13**, 517–522, https://doi.org/10.1080/00167616608728629

Trendall, A.F. 1991. The 'Geological Unit' (g.u.) – A suggested new measure of geologic time. *Geology*, **19**, 195, https://doi.org/10.1130/0091-7613(1991)019<0195:TGUGUA>2.3.CO;2

Trendall, A.F., Compston, W., Nelson, D.R., De Laeter, J.R. and Bennett, V.C. 2004. SHRIMP zircon ages constraining the depositional chronology of the Hamersley Group, Western Australia. *Australian Journal of Earth Sciences*, **51**, 621–644, https://doi.org/10.1111/j.1400-0952.2004.01082.x

Tsikos, H., Matthews, A., Erel, Y. and Moore, J.M. 2010. Iron isotopes constrain biogeochemical redox cycling of iron and manganese in a Palaeoproterozoic stratified basin. *Earth and Planetary Science Letters*, **298**, 125–134, https://doi.org/10.1016/j.epsl.2010.07.032

Van Kranendonk, M.J. 2011. Stromatolite morphology as an indicator of biogenicity for Earth's oldest fossils from the 3.5–3.4 Ga Pilbara Craton, Western Australia. *In*: Reitner, J., Queric, N.-V. and Arp, G. (eds) *Advances in Stromatolite Geobiology*. Lecture Notes in Earth Sciences, **131**, 200.

Van Kranendonk, M.J. and Kirkland, C.L. 2016. Conditioned duality of the Earth system: Geochemical tracing of the supercontinent cycle through Earth history. *Earth-Science Reviews*, **160**, 171–187, https://doi.org/10.1016/j.earscirev.2016.05.009

Van Kranendonk, M.J., Webb, G.E. and Kamber, B.S. 2003. Geological and trace element evidence for a marine sedimentary environment of deposition and biogenicity of 3.45 Ga stromatolitic carbonates in the Pilbara Craton, and support for a reducing Archaean ocean. *Geobiology*, **1**, 91–108, https://doi.org/10.1046/j.1472-4669.2003.00014.x

Van Kranendonk, M.J., Collins, W.J., Hickman, A. and Pawley, M.J. 2004. Critical tests of vertical vs. horizontal tectonic models for the Archaean Pilbara granite-greenstone terrane, Pilbara craton, western Australia. *Precambrian Research*, **131**, 173–211, https://doi.org/10.1016/j.precamres.2003.12.015

Van Kranendonk, M.J., Altermann, W., *et al.* 2012. A chronostratigraphic division of the Precambrian: possibilities and challenges. *In*: Gradstein, F.M., Ogg, J.G., Schmitz, M. and Ogg, G. (eds) (Coords). *The Geologic Time Scale 2012*. Elsevier, 299–392.

Veizer, J. 1989. Strontium isotopes in seawater through time. *Annual Reviews of Earth and Planetary Sciences*, **17**, 141–167, https://doi.org/10.1146/annurev.ea.17.050189.001041

Vermeesch, P., Resentini, A. and Garzanti, E. 2016. An R package for statistical provenance analysis. *Sedimentary Geology*, **336**, 14–25. https://doi.org/10.1016/j.sedgeo.2016.01.009

Walter, M.R., Oehler, J.H. and Oehler, D.Z. 1976. Megascopic algae 1300 million years old from the Belt Supergroup, Montana: a reinterpretation of Walcott's Helminthoidichnites. *Journal of Paleontology*, **50**, 872–881.

Wan, B., Yang, X., Tian, X., Yuan, H., Kirscher, U. and Mitchell, R.N. 2020. Seismological evidence for the earliest global subduction network at 2 Ga. *Science Advances*, **6**, eabc5491, https://doi.org/10.1126/sciadv.abc5491

Wang, C., Peng, P., Wang, X. and Yang, S. 2016. Nature of three Proterozoic (1680, 1230 and 775 Ma) mafic dyke swarms in North China: Implications for tectonic evolution and paleogeographic reconstruction. *Precambrian Research*, **285**, 109–126, https://doi.org/10.1016/j.precamres.2016.09.015

Wang, D., Zhu, X.-K., Zhao, N., Yan, B., Li, X.-H., Shi, F. and Zhang, F. 2019. Timing of the termination of Sturtian glaciation: SIMS U–Pb zircon dating from South China. *Journal of Asian Earth Sciences*, **177**, 287–294, https://doi.org/10.1016/j.jseaes.2019.03.015

Wang, X.C., Li, Z.X., Li, X.H., Li, Q.L. and Zhang, Q.-R. 2011. Geochemical and Hf-Nd isotope data of Nanhua rift sedimentary and volcaniclastic rocks indicate a Neoproterozoic continental flood basalt provenance. *Lithos*, 427–440, https://doi.org/10.1016/j.lithos.2011.09.020

Warke, M.R., Strauss, H. and Schröder, S. 2020*a*. Positive cerium anomalies imply pre-GOE redox stratification and manganese oxidation in Paleoproterozoic shallow marine environments. *Precambrian Research*, **344**, 105767, https://doi.org/10.1016/j.precamres.2020.105767

Warke, M.R., Di Rocco, T., *et al.* 2020*b*. The Great Oxidation Event preceded a Paleoproterozoic Snowball Earth. *Proceedings of the National Academy of Sciences*, **117**, 13314–13320, https://doi.org/10.1073/pnas.2003090117

Whitmeyer, S.J. and Karlstrom, K.E. 2007. Tectonic model for the Proterozoic growth of North Americ. *Geosphere*, **3**, 220–259, https://doi.org/10.1130/GES00055.1

Worsley, T.R., Nance, R.D. and Moody, J.B. 1985. Proterozoic to recent tectonic tuning of biogeochemical cycles. *In*: Sunquist, E.T. and Broecker, W.S. (eds) *The Carbon Cycle and Atmospheric CO_2: Natural Variations Archean to Present*. American Geophysical Union, Geophysical Monographs, **32**, 561–572.

Xiao, S. and Narbonne, G.M. 2020. The Ediacaran Period. *In*: Gradstein, F.M., Ogg, J.G., Schmitz, M.D. and Ogg, G.M. (eds) *The Geologic Time Scale 2020*. Elsevier Science, **1**, 521–560.

Xiao, S. and Tang, Q. 2018. After the boring billion and before the freezing millions: evolutionary patterns and innovations in the Tonian Period. *Emerging Topics in Life Sciences*, **2**, 161–171, https://doi.org/10.1042/ETLS20170165

Yang, B., Collins, A.S., Blades, M.L., Capogreco, N., Payne, J.L., Munson, T.J. and Cox, G.M. 2019. Middle-late Mesoproterozoic tectonic geography of the North Australia Craton: U–Pb and Hf isotopes of detrital zircons in the Beetaloo Sub-basin, Northern Territory, Australia. *Journal of the Geological Society, London*, **176**, 771–784, https://doi.org/10.1144/jgs2018-159

Yang, B., Collins, A.S. *et al.* 2020. Using Mesoproterozoic Sedimentary Geochemistry to Reconstruct Basin Tectonic Geography and Link Organic Carbon Productivity to Nutrient Flux from a Northern Australian Large Igneous Province. *Basin Research*, **32**, 1734–1750, https://doi.org/10.1111/bre.12450

Yin, L. 1997. Acanthomorphic acritarchs from Meso-Neoproterozoic shales of the Ruyang Group, Shanxi, China. *Review of Palaeobotany and Palynology*, **98**, 15–25, https://doi.org/10.1016/S0034-6667(97)00022-5

Yin, L., Changtai, N. and Kong, F.-F. 2018. A review of Proterozoic organic walled microfossils – *Tappania* and its biologic and geologic implication. *Acta Palaeontology Sinica*, **57**, 147–156.

Young, G.M. 2013. Precambrian supercontinents, glaciations, atmospheric oxygenation, metazoan evolution and an impact that may have changed the second half of Earth history. *Geoscience Frontiers*, **4**, 247–261, https://doi.org/10.1016/j.gsf.2012.07.003

Young, G.M. 2019. Aspects of the Archean–Proterozoic transition: How the great Huronian Glacial Event was initiated by rift-related uplift and terminated at the rift-drift transition during break-up of Lauroscandia. *Earth Science Reviews*, **190**, 171–189, https://doi.org/10.1016/j.earscirev.2018.12.013

Zalasiewicz, J., Smith, A., *et al.* 2004. Simplifying the stratigraphy of time. *Geology*, **32**, 1–4, https://doi.org/10.1130/G19920.1

Zhai, M.G., Hu, B., Zhao, T.P., Peng, P. and Meng, Q.R. 2015. Late Paleoproterozoic–Neoproterozoic multi-rifiting events in the North China craton and their geological significance: a study advance and review. *Tectonophysics*, **662**, 153–166, https://doi.org/10.1016/j.tecto.2015.01.019

Zhang, K., Zhu, X., Wood, R., Shi, Y., Gao, Z. and Poulton, S.W. 2018. Oxygenation of the Mesoproterozoic ocean and the evolution of complex eukaryotes. *Nature Geoscience*, **11**, 345–350, https://doi.org/10.1038/s41561-018-0111-y

Zhang, S., Li, Z., Evans, D.A.D., Wu, H., Li, H. and Dong, J. 2012. Pre-Rodinia supercontinent Nuna shaping up: A global synthesis with new paleomagnetic results from North China. *Earth and Planetary Science Letters*, **353–354**, 145–155, https://doi.org/10.1016/j.epsl.2012.07.034

Zhang, S.H., Zhao, Y., Li, X.H., Ernst, R.E. and Yang, Z.Y. 2017. The 1.33–1.30 Ga Yanliao large igneous province in the North China Craton: Implications for reconstruction of the Nuna (Columbia) supercontinent, and specifically with the North Australian Craton. *Earth and Planetary Science Letters*, **465**, 112–125, https://doi.org/10.1016/j.epsl.2017.02.034

Zhang, S.H., Ernst, R.E., Pei, J., Zhao, Y., Zhou, M. and Hu, G. 2018. A temporal and causal link between c. 1380 Ma large igneous provinces and black shale: Implications for the Mesoproterozoic time scale and paleoenvironment. *Geology*, **46**, 963–966, https://doi.org/10.1130/G45210.1

Zhao, G. and Cawood, P.A. 2012. Precambrian geology of China. *Precambrian Research*, **222–223**, 13–54, https://doi.org/10.1016/j.precamres.2012.09.017

Zhao, G., Cawood, P.A., Wilde, S.A. and Sun, M. 2002. Review of global 2.1–1.8 Ga orogens: implications for a pre-Rodinia supercontinent. *Earth-Science Reviews*, **59**, 125–162, https://doi.org/10.1016/S0012-8252(02)00073-9

Zhou, C.M., Huyskens, M.H., Lang, X.G., Xiao, S.H. and Yin, Q.Z. 2019. Calibrating the terminations of Cryogenian global glaciations. *Geology*, **47**, 251–254, https://doi.org/10.1130/G45719.1

Zhou, Y., Pogge von Strandmann, P.A.E., *et al.* 2020. Reconstructing Tonian seawater $^{87}Sr/^{86}Sr$ using calcite microspar. *Geology*, **48**, 462–467, https://doi.org/10.1130/G46756.1

Zhu, S., Zhu, M., *et al.* 2016. Decimetre-scale multicellular eukaryotes from the 1.56-billion-year-old Gaoyuzhuang Formation in North China. *Nature Communications*, https://doi.org/10.1038/ncomms11500

Zumberge, J.A., Rocher, D. and Love, G.D. 2020. Free and kerogen-bound biomarkers from late Tonian sedimentary rocks record abundant eukaryotes in mid-Neoproterozoic marine communities. *Geobiology*, **18**, 326–347, https://doi.org/10.1111/gbi.12378